

Electronic Thesis and Dissertation Repository

---

8-22-2019 1:00 PM

## The role of ATF4 in amyloid-beta-induced neuronal death.

Gillian Petroff, *The University of Western Ontario*

Supervisor: Cregan, Sean P., *The University of Western Ontario*

A thesis submitted in partial fulfillment of the requirements for the Master of Science degree in  
Physiology and Pharmacology

© Gillian Petroff 2019

Follow this and additional works at: <https://ir.lib.uwo.ca/etd>



Part of the [Neurosciences Commons](#)

---

### Recommended Citation

Petroff, Gillian, "The role of ATF4 in amyloid-beta-induced neuronal death." (2019). *Electronic Thesis and Dissertation Repository*. 6377.

<https://ir.lib.uwo.ca/etd/6377>

This Dissertation/Thesis is brought to you for free and open access by Scholarship@Western. It has been accepted for inclusion in Electronic Thesis and Dissertation Repository by an authorized administrator of Scholarship@Western. For more information, please contact [wlsadmin@uwo.ca](mailto:wlsadmin@uwo.ca).

## Abstract

Alzheimer's disease (AD) is partially characterized by excessive accumulation of amyloid- $\beta$  ( $A\beta$ ) in the brain.  $A\beta$  oligomers have greater toxicity than  $A\beta$  fibrils and induce neuronal stress. The Integrated Stress Response (ISR) is activated in response to cellular stress and increases expression of activating transcription factor 4 (ATF4) and its target genes. Prolonged activation has been shown to induce aberrant cell death, and increased markers of the ISR have been found in the brains of AD patients. However, the exact mechanism of amyloid- $\beta$ -induced death is largely unknown. We aimed to determine if  $A\beta$ -induced neuronal death occurs through ATF4-mediated upregulation of its downstream pro-apoptotic gene PUMA. Primary cortical neurons were treated with  $A\beta$  oligomers.  $A\beta$  induced apoptosis in a PUMA-dependent manner in the presence of ATF4. These results suggest that therapeutics targeting ATF4 and PUMA may be successful in alleviating excessive neuronal death induced by amyloid- $\beta$  in Alzheimer's disease.

## Keywords

Amyloid- $\beta$ , Integrated Stress Response, Activating Transcription Factor 4, ATF4, Apoptosis, PUMA

## Lay Summary

Alzheimer's disease (AD) is the most common type of dementia. AD is a degenerative disease affecting the brain. As the disease progresses, brain cells continually die. One of the main proteins that is involved in the development of AD is amyloid- $\beta$ . When levels of amyloid- $\beta$  are elevated in the brain, the proteins tend to aggregate together. These clumps are harmful to brain cells, which are also called neurons. Amyloid- $\beta$  can cause high levels of stress in neurons. The Integrated Stress Response (ISR) is a pathway within cells that helps them to overcome a wide range of stress signals. When the ISR detects stress in the environment, it becomes activated and increases the expression of another protein called Activating Transcription Factor 4 (ATF4). ATF4 helps increase the production of proteins that can help the cell mediate the stress and return back to normal. However, sustained activation of the ISR has been shown to promote death signals within cells. High levels of many ISR proteins have been found in the brains of AD patients. The way in which amyloid- $\beta$  causes neuronal death remains largely unknown. We aimed to determine if amyloid- $\beta$  causes neuronal death through prolonged activation of ATF4 and increased expression of the pro-death protein PUMA. In the present study, neurons were treated with amyloid- $\beta$  aggregates. Amyloid- $\beta$  induced neuronal death in the presence of both ATF4 and PUMA. When ATF4 or PUMA were removed from these neurons, amyloid- $\beta$  did not cause death. The results suggest that drugs targeting ATF4 and PUMA may be successful in reducing neuronal death caused by amyloid- $\beta$  in Alzheimer's disease.

## Acknowledgments

Firstly, I would like to thank my supervisor Dr. Sean Cregan. I am honoured and grateful for all of the support he has given me throughout the past two years. His encouragement and guidance have helped shaped me into the scientist I always aspired to be. There are not many supervisors who spend as much time in the lab with their students as he does. It was reassuring to know I always had the support to work through any problems I came across. I want to thank him for giving me wonderful opportunities to present my research at numerous conferences. The SfN conference in San Diego was not only a lot of fun, but it helped grow my confidence as a researcher. Without Dr. Cregan believing in me, none of this would have been possible. I would also like to thank the members of my advisory committee, Dr. John Di Guglielmo, Dr. Vania Prado, and Dr. Wataru Inoue, for providing guidance and helping shape my project into the final product.

To my amazing lab members, I could not have made it this far without your support. Heather, Matt, Elizabeth, Lauren, Fatemeh and Vidhya, thank you for making this experience unforgettable. You provided me with so much emotional and technical support throughout this journey and I am so grateful to have met each one of you. We are more than just colleagues; we are lifelong friends.

Lastly, and most importantly, I would like to thank my incredible parents, Howie and Andrea. I owe this wonderful experience to you and your unconditional love and support. I am extremely lucky to have so many amazing people in my life. To my brothers, Alex, the rest of my family, and all of my friends, thank you for supporting my dream and encouraging me when I doubted myself.

I would not be who I am today without all of the people mentioned above, and I am forever grateful.



# Table of Contents

Abstract.....	i
Lay Summary.....	ii
Acknowledgments.....	iii
Table of Contents.....	iv
List of Figures.....	vii
List of Appendices.....	viii
List of Abbreviations.....	ix
Chapter 1.....	1
1 Introduction.....	1
1.1 Alzheimer’s disease.....	1
1.1.1 Amyloid- $\beta$ .....	2
1.2 The Integrated Stress Response.....	6
1.2.1 Activating Transcription Factor 4.....	9
1.2.2 ISR and Apoptosis.....	14
1.3 The ISR in Alzheimer’s disease.....	15
1.3.1 Cellular stress in AD.....	15
1.3.2 ISR and Memory.....	17
1.4 Rationale.....	19
1.5 Hypothesis.....	19
Chapter 2.....	20
2 Materials and Methods.....	20
2.1 Animals.....	20
2.1.1 Genotyping.....	20
2.2 Cell culture.....	21

2.2.1	Primary cortical neurons .....	21
2.2.2	Drugs.....	22
2.3	Protein extraction and quantification .....	25
2.4	RNA isolation and quantification .....	25
2.5	Western blot analysis .....	25
2.6	Real-time quantitative RT-PCR analysis .....	26
2.7	Cell death assay.....	26
2.8	Caspase-3 activity assay .....	27
2.9	Fluorescent immunocytochemistry .....	28
2.10	Data analysis .....	28
Chapter 3	.....	29
3	Results .....	29
3.1	Amyloid- $\beta$ activates the ISR <i>in vitro</i> .....	29
3.2	Amyloid- $\beta$ increases pro-apoptotic gene expression .....	31
3.3	Amyloid- $\beta$ induces neuronal apoptosis .....	32
3.3.1	Amyloid- $\beta$ -induced toxicity is sequence specific.....	35
3.4	ATF4-deficiency attenuates pro-apoptotic gene expression.....	38
3.5	Apoptosis is attenuated in ATF4-deficient neurons.....	40
3.6	PUMA mediates neuronal apoptosis in an ATF4-dependent manner .....	43
3.6.1	Amyloid- $\beta$ induces ATF4-dependent PUMA expression.....	43
3.6.2	Caspase-mediated apoptosis is attenuated in PUMA-deficient neurons...	45
Chapter 4	.....	48
4	Discussion .....	48
4.1	Oligomeric Amyloid- $\beta$ induces ATF4 expression and apoptosis in neurons .....	48
4.2	ATF4 is necessary for amyloid- $\beta$ -induced neuronal death.....	50

4.3 Amyloid- $\beta$ -induced death occurs through ATF4-mediated upregulation of PUMA .....	51
4.4 Implications of ATF4 in Alzheimer's disease .....	52
Chapter 5.....	53
5 Conclusion.....	53
References.....	55
Appendices.....	74
Curriculum Vitae .....	77

## List of Figures

Figure 1.1. Amyloid precursor protein processing. ....	3
Figure 1.2. The Integrated Stress Response.....	8
Figure 1.3. Functional domains of the ATF4 protein. ....	11
Figure 2.1. Oligomeric and scrambled amyloid- $\beta$ peptides.....	24
Figure 3.1. Oligomeric amyloid- $\beta$ induces ATF4 expression. ....	30
Figure 3.2. Amyloid- $\beta$ induces pro-apoptotic gene expression.....	33
Figure 3.3. Oligomeric amyloid- $\beta$ induces neuronal apoptosis.....	34
Figure 3.4. Scrambled amyloid- $\beta$ does not induce cellular stress. ....	36
Figure 3.5. Pro-apoptotic gene expression is attenuated in ATF4-deficient neurons. ....	39
Figure 3.6. ATF4 is necessary for amyloid- $\beta$ -induced apoptosis. ....	42
Figure 3.7. PUMA expression is attenuated in ATF4-deficient neurons.....	44
Figure 3.8. Amyloid- $\beta$ -induced cell death occurs in a PUMA-dependent manner. ....	47
Figure 5.1. Schematic of amyloid- $\beta$ -induced neuronal apoptosis. ....	54

## List of Appendices

Appendix A: ATF4 genotyping primers .....	74
Appendix B: PUMA genotyping primers .....	75
Appendix C: List of qRT-PCR primers .....	76

## List of Abbreviations

4eBP1	eukaryotic initiation factor 4E-binding protein 1
AARE	amino acid response element
A $\beta$	amyloid beta
AD	Alzheimer's disease
AFU	arbitrary fluorescence unit
AICD	amyloid precursor protein intracellular domain
ANOVA	analysis of variance
APAF1	apoptotic protease-activating factor-1
APH1	anterior pharynx-defective 1
ApoE	apolipoprotein E
APP	amyloid precursor protein
APP/PS-1	amyloid precursor protein/presenilin-1
ATF4	activating transcription factor 4
$\beta$ -TrCP	$\beta$ -transducin repeats containing protein
BACE1	$\beta$ -site APP cleaving enzyme
BAK	Bcl-2 homologous antagonist killer

BAX	Bcl-2 associated X protein
BCA	bicinchoninic acid
BCL-2	B-cell lymphoma-2
BH3	Bcl-2 homology domain-3
BiP	binding immunoglobulin protein
BSA	bovine serum albumin
bZIP	basic leucine zipper
CARE	C/EBP-ATF response element
C/EBP	CCAAT enhancer binding protein
CHOP	CCAAT-homologous protein
CRE	cAMP responsive element
CREB	cAMP responsive element binding protein
CREB-2	cAMP response element binding protein 2
CTF $\alpha$	C-terminal fragment $\alpha$
CTF $\beta$	C-terminal fragment $\beta$
ddH <sub>2</sub> O	double distilled water
DIV	days in vitro

DMSO	dimethylsulfoxide
DNA	deoxyribonucleic acid
dNTP	deoxyribonucleotide triphosphate
DTT	dithiothreitol
EC	entorhinal cortex
EDTA	Ethylenediaminetetraacetic acid
eIF2 $\alpha$	eukaryotic initiation factor 2 alpha
eIF5	eukaryotic initiation factor 5
ER	endoplasmic reticulum
FAD	familial Alzheimer's disease
Gadd34	growth arrest and DNA damage-inducible protein 34
Gadd45 $\alpha$	growth arrest and DNA damage-inducible protein 45 alpha
GCN2	general control non-derepressible 2
GDP	guanine diphosphate
GEF	guanine exchange factor
Grp78	78-kDa glucose-related protein
GTP	guanine triphosphate



HBSS	hank's balanced salt solution
HFIP	1,1,1,3,3,3-hexafluoro-2-propanol
HRI	heme-regulated eukaryotic initiation factor-2 $\alpha$ kinase
ISR	integrated stress response
KO	knockout
LTP	long-term potentiation
MEF	mouse embryonic fibroblast
mRNA	messenger ribonucleic acid
NBM	neurobasal plus medium
NEP	neprilysin
ODDD	oxygen-dependent degradation domain
OMM	outer mitochondrial membrane
PBS	phosphate buffered saline
PCR	polymerase chain reaction
PEN2	presenilin enhancer 2
PERK	PKR-like endoplasmic reticulum kinase
PFA	paraformaldehyde

PIC	preinitiation complex
PHD3	prolyl hydroxylase domain 3
PKR	double stranded RNA-dependent protein kinase
PP1	protein phosphatase 1
PS1	presenilin 1
PS2	presenilin 2
PUMA	p53-upregulated modulator of apoptosis
PVDF	polyvinylidene difluoride
qRT-PCR	quantitative real-time polymerase chain reaction
RIPA	radioimmunoprecipitation assay
RNA	ribonucleic acid
SAD	sporadic Alzheimer's disease
SDS	Sodium dodecyl sulfate
SDS-PAGE	sodium dodecyl sulfate polyacrylamide gel
SEM	standard error of the mean
TBST	tris buffered saline – tween 20
TC	ternary complex

TG	thapsigargin
Trib3	tribbles pseudokinase 3
tRNA	transfer ribonucleic acid
uORF	upstream open reading frame
UT	untreated
WT	wildtype

## Chapter 1

### 1 Introduction

#### 1.1 Alzheimer's disease

Alzheimer's disease (AD) is the most common form of dementia (Chambers, Bancej, & McDowell, 2016). It is characterized by a progressive loss in hippocampal and total brain mass, coupled with increasing memory loss and behavioural changes, that can ultimately result in death (Nelson, Braak, & Markesbery, 2009). Currently, it is estimated that close to 600,000 Canadians live with dementia (Chambers et al., 2016). Caring for those with AD poses a large financial burden on our healthcare system, with annual costs close to \$10 billion (Chambers et al., 2016). With an aging population, these numbers will only rise, which highlights the relevance of dementia research.

One of the most common behavioural symptoms of Alzheimer's disease is memory impairment that affects daily functioning. It is often the earliest manifestation of the disease that is noticed by patients and their families. Other behavioural symptoms include difficulties with language and changes in personality (Chambers et al., 2016).

Pathologically, AD is characterized by two main hallmarks: amyloid plaques and neurofibrillary tangles. Amyloid plaques are composed of extracellular aggregates of amyloid- $\beta$  protein. Neurofibrillary tangles are composed of hyperphosphorylated tau protein that has aggregated intracellularly (Joshi, Kornfeld, & Mochly-Rosen, 2016; Nelson et al., 2009).

In Alzheimer's disease, pathological changes occur prior to the development of clinical symptoms. Pathology generally begins in the entorhinal cortex (EC) in the temporal lobe, progresses through the limbic system, and gradually spreads throughout the cortex (Braak & Braak, 1991; Masliah et al., 1994). The entorhinal cortex has synaptic connections with structures such as the hippocampus, which highlights its importance as a hub for Alzheimer's disease progression (Harris et al., 2010). The hippocampus is a structure that is important for memory, and correlations between hippocampal volume and cognitive testing scores in AD patients have been established (Farrow et al., 2007). More

specifically, in early AD, smaller hippocampal volumes correlated with worse performance on cognitive tests. In addition to volumetric differences, decreased synapse numbers in the EC and hippocampus have been found in patients with early Alzheimer's disease compared to mild cognitive impairment and normal aging (Scheff, Price, Schmitt, & Mufson, 2006). This lowered number of synapses was correlated with lower cognitive testing scores.

### 1.1.1 Amyloid- $\beta$

Amyloid- $\beta$  (A $\beta$ ) peptide is generated from the sequential proteolytic cleavage of the amyloid precursor protein (APP; Chen et al., 2017; Kang et al., 1987). APP is located on the plasma membrane and contains a single transmembrane domain, along with an intracellular C-terminus and a large extracellular N-terminus (Figure 1.1). It can be processed through two proteolytic pathways: a non-amyloidogenic pathway and an amyloidogenic pathway (Chen et al., 2017; Kang et al., 1987; Selkoe, 1994). The non-amyloidogenic pathway occurs when APP is first cleaved by  $\alpha$ -secretase, which releases the N-terminus into the extracellular environment. The cleavage site for  $\alpha$ -secretase lies within the amyloid- $\beta$  sequence, and thus prevents pathologic amyloid- $\beta$  production. The membrane-bound C-terminus (CTF $\alpha$ ) is subsequently cleaved by  $\gamma$ -secretase, which then releases extracellular P3 and APP intracellular domain (AICD; Chen et al., 2017; Olsson et al., 2014). For processing through the amyloidogenic pathway, APP is cleaved by  $\beta$ -secretase, also termed  $\beta$ -site APP cleaving enzyme (BACE1). Cleavage by  $\beta$ -secretase releases the extracellular N-terminal fragment and leaves the membrane-tethered C-terminal fragment (CTF $\beta$ ). CTF $\beta$  is subsequently cleaved by  $\gamma$ -secretase to generate AICD and amyloid- $\beta$  peptide (Murphy & Levine, 2010; Olsson et al., 2014).  $\gamma$ -secretase can cleave CTF $\beta$  at many different sites, generating amyloid- $\beta$  species of varying lengths (Haass & Selkoe, 2007; Olsson et al., 2014; Takami et al., 2009). Amyloid- $\beta$  can be released into the extracellular space or associate with lipid rafts to become internalized (Chen et al., 2017).

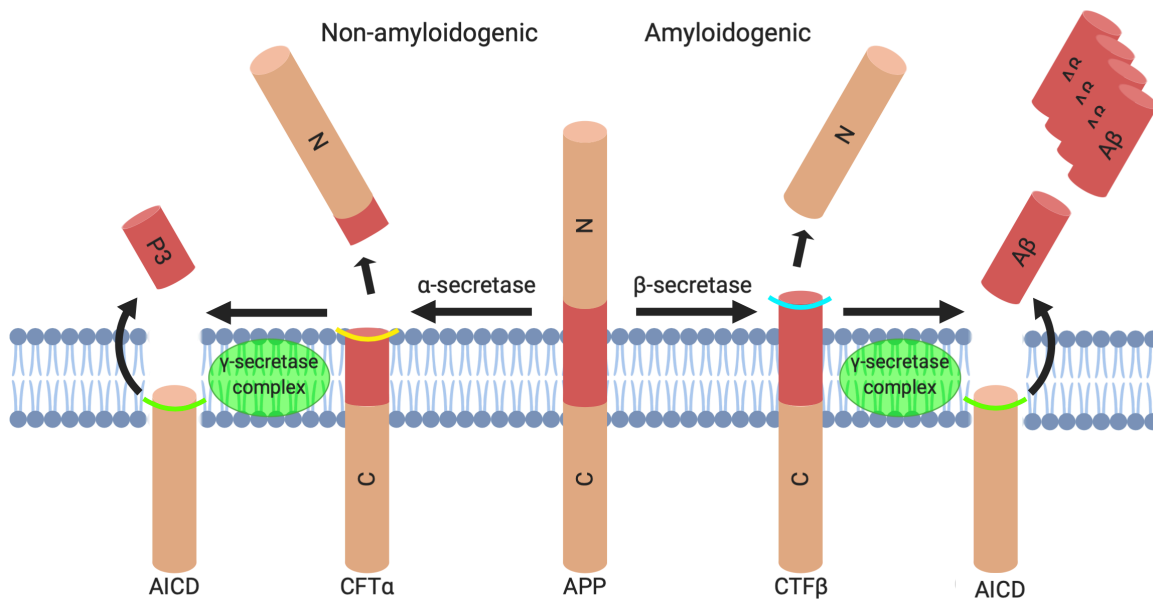


**Figure 1.1. Amyloid precursor protein processing.** Amyloid precursor protein (APP) can be processed through the non-amyloidogenic or amyloidogenic cleavage pathways. Through the non-amyloidogenic pathway, APP is first cleaved by  $\alpha$ -secretase at a cleavage site within the amyloid- $\beta$  sequence. The N-terminus is then released into the extracellular environment. The remaining C-terminus embedded in the membrane is then cleaved by  $\gamma$ -secretase, releasing P3 and AICD into the extracellular and intracellular environments, respectively. When APP is processed through the amyloidogenic pathway, it is first cleaved by  $\beta$ -secretase, releasing the N-terminus into the extracellular space. The remaining C-terminal fragment (CTF $\beta$ ) is sequentially cleaved by  $\gamma$ -secretase. AICD and A $\beta$  peptides are then released. A $\beta$  peptides of a certain length have a propensity to aggregate and can become pathological in nature.

Despite the known pathological effects of amyloid- $\beta$ , APP and A $\beta$  also have physiological roles. The production of amyloid- $\beta$  is naturally occurring, however when the net levels of amyloid- $\beta$  become extreme, it becomes pathological in nature (Pearson & Peers, 2006). Amyloid- $\beta$  is produced during normal metabolism in cultured primary cells and cell lines (Haass et al., 2003). APP and its cleaved protein fragments have been posited to play important roles in processes such as neuronal survival and synaptic activity. For example, synaptic activity has been shown to increase the production of amyloid- $\beta$ , which creates a negative feedback loop and inhibits further synaptic activity (Lesne et al., 2005). The proposed explanation for the beneficial effects of synaptic inhibition is by controlling excessive glutamate release and protecting against excitotoxicity (Lesne et al., 2005). Additionally, in cortical neurons, the N-terminus released extracellularly following APP cleavage by  $\alpha$ -secretase has been shown to promote cell survival and neurite extensions (Araki et al., 1991). Despite these pro-survival roles of APP and amyloid- $\beta$ , aberrant production and excessive protein levels are present in AD and are detrimental to cells.

There are many mutations in the APP gene, located on chromosome 21, that result in preferential processing of APP through the amyloidogenic pathway (Haass et al., 1995; Rozpedek, Markiewicz, Diehl, Pytel, & Majsterek, 2015). These mutations occur around the  $\beta$ - and  $\gamma$ -secretase cleavage sites and can lead to familial Alzheimer's disease (FAD; Haass et al., 1995). Mutations near the  $\beta$ -secretase cleavage site lead to increased processing of APP through the amyloidogenic pathway, and mutations near the  $\gamma$ -secretase cleavage site lead to the generation of longer amyloid- $\beta$  species (Haass et al., 1995; Scheuner et al., 1996). These longer species of amyloid- $\beta$ , such as A $\beta_{42}$ , are more prone to aggregation than shorter fragments, such as A $\beta_{40}$  (Bentahir et al., 2006; Wakabayashi & De Strooper, 2008).

In addition to mutations in the APP gene, there are mutations within the  $\gamma$ -secretase enzyme that can alter APP processing.  $\gamma$ -secretase is a multi-subunit enzyme composed of presenilin (PS1 or PS2), nicastrin, anterior pharynx-defective 1 (APH1), and presenilin enhancer 2 (PEN2; De Strooper, 2003; Haass & Selkoe, 1993; Iwatsubo, 2004; Kimberly

et al., 2003). Presenilin is believed to form the active site of this protein complex, and nicastrin helps to dock the protein substrate (Kimberly et al., 2003; Wakabayashi & De Strooper, 2008). There are over 200 identified mutations in both PS1 and PS2 combined that can alter its enzymatic activity (<http://www.molgen.ua.ac.be/ADMutations/>).  $\gamma$ -secretase has the ability to cleave the CFT $\beta$  fragment at many sites, which generates amyloid- $\beta$  peptides of varying lengths (Olsson et al., 2014). Mutations in the presenilin genes have been shown to increase CFT $\beta$  cleavage into longer A $\beta$  fragments (Scheuner et al., 1996).

Amyloid- $\beta$  can aggregate into a fibrillar or an oligomeric form (Deshpande, Mina, Glabe, & Busciglio, 2006; Gouras, Olsson, & Hansson, 2015). Amyloid plaques are composed mainly of insoluble fibrillar amyloid- $\beta$  peptides; however, it is thought that soluble oligomeric amyloid- $\beta$  is more toxic to neurons than the fibrillar form (Deshpande et al., 2006). It has been shown that soluble A $\beta_{42}$  aggregates into oligomers more readily than A $\beta_{40}$ , due to the residues present at its C-terminus (Bitan et al., 2002; Murphy & Levine, 2010). The total A $\beta_{42}$  burden present, as well as the ratio of A $\beta_{42}$ /A $\beta_{40}$ , factor into the age of disease onset (Chen et al., 2017; Duering, Grimm, Grimm, Schröder, & Hartmann, 2005). Soluble amyloid- $\beta$  aggregates have a heterogenous size distribution (Bitan et al., 2002; Haass & Selkoe, 2007). Oligomers can be on the order of small molecular weights, such as dimers, trimers, and tetramers, and up to midrange molecular weights, such as hexamers and nonamers (Bitan et al., 2002; Chen et al., 2017).

The clearance of amyloid- $\beta$  is an important process that can be altered in Alzheimer's disease. Several processes are naturally in place to counterbalance the production of A $\beta$  (Caccamo, Oddo, Sugarman, Akbari, & LaFerla, 2005; Iwata et al., 2000; Miners et al., 2006; Yasojima, Akiyama, McGeer, & McGeer, 2001). Processes such as extracellular proteolytic degradation, endocytosis followed by intracellular proteolytic degradation, and transport out of the brain, are examples of potential mechanisms that are used (Chen et al., 2017; Iwata et al., 2000). Neprilysin (NEP) is a type 2 membrane glycoprotein that is the most efficient peptidase of amyloid- $\beta$  (Iwata et al., 2000). It can be localized to cellular compartments such as the Golgi and endoplasmic reticulum (ER), and its active



site is located in the intraluminal and extracellular spaces (Chen et al., 2017). Interestingly, levels of neprilysin have been shown to be reduced in an age-dependent manner. In the hippocampi of AD patients, as well as in mouse models of Alzheimer's disease, levels of neprilysin are significantly attenuated compared to controls (Caccamo et al., 2005; Miners et al., 2006; Yasojima et al., 2001). The relationship between amyloid- $\beta$  production and clearance is an important balance to maintain, because perturbations in this system can lead to or accelerate the progression of Alzheimer's disease.

## 1.2 The Integrated Stress Response

The Integrated Stress Response (ISR) is a conserved, adaptive pathway that allows cells to respond to and mitigate various environmental stresses (Pakos-Zebrucka et al., 2016; Ron, 2002). These stress stimuli can be both intrinsic, such as endoplasmic reticulum stress, or extrinsic, for example amino acid or glucose deprivation (Harding et al., 2003; Pakos-Zebrucka et al., 2016; Ron, 2002). The ISR begins with four protein kinases that each detect a specific type of stressor. These kinases are heme-regulated eukaryotic initiation factor-2 $\alpha$  kinase (HRI), double stranded RNA-dependent protein kinase (PKR), PKR-like endoplasmic reticulum kinase (PERK), and general control non-derepressible 2 (GCN2; Chen et al., 2011; Onuki et al., 2004; Pakos-Zebrucka et al., 2016; Szegezdi, Logue, Gorman, & Samali, 2006; Ye et al., 2010). Excluding HRI, the ISR kinases are highly expressed in the mammalian brain (Ohno, 2014). The ISR kinases have conserved catalytic kinase domains and distinct regulatory domains, which allows for the detection of numerous stressors (J. J. Chen et al., 1991; Donnelly, Gorman, Gupta, & Samali, 2013). PERK is a transmembrane protein that lies on the endoplasmic reticulum membrane and detects ER stress. Increased levels of unfolded or misfolded proteins and disruptions in calcium homeostasis are some of the stimuli that can induce ER stress (Carrara, Prischi, Nowak, Kopp, & Ali, 2015; Moore, Omikorede, Gomez, Willars, & Herbert, 2011; Pakos-Zebrucka et al., 2016). PKR was initially discovered to become activated by viral infection, and subsequent research has determined that PKR also responds to more general stress signals, such as ER and oxidative stress (Onuki et al., 2004). GCN2 mainly senses the availability of amino acids and becomes activated during

amino acid deprivation (Deval et al., 2009). Once a stressor has been detected, the corresponding kinase will dimerize and autophosphorylate, thus becoming active. The kinases converge by phosphorylating the  $\alpha$ -subunit of eukaryotic initiation factor-2 (eIF2 $\alpha$ ) at serine 51 (Figure 1.2; Baird & Wek, 2012; Ron, 2002).

eIF2 is a heterotrimeric protein and it is composed of an  $\alpha$ ,  $\beta$ , and  $\gamma$  subunit. It aids in the initiation of cap-dependent protein translation (Kimball, 1997). The  $\alpha$  subunit of eIF2 contains the regulatory phosphorylation site. Under non-phosphorylated conditions, eIF2 binds with GTP and initiator methionine tRNA (Met-tRNA<sub>i</sub>) to form the ternary complex (TC). The ternary complex then binds to the 40S ribosomal subunit, along with a few more initiation factors, to form the 43S pre-initiation complex (PIC; Hinnebusch & Lorsch, 2012). The 43S PIC is recruited to the 5' cap of the mRNA transcript and begins scanning for the AUG start codon. Once the Met-tRNA<sub>i</sub> binds to the AUG start codon, eIF2-GTP is hydrolyzed to eIF2-GDP with the help of eIF5 (Das, Maiti, Das, & Maitra, 1997). eIF2-GDP disassociates from the 40S ribosomal complex and allows for the 60S ribosomal subunit to be recruited and begin translation elongation. GDP-bound eIF2 is inactive and needs to be recycled back into eIF2-GTP in order to be able to facilitate a new round of translation initiation (Krishnamoorthy, Pavitt, Zhang, Dever, & Hinnebusch, 2001). This recycling is aided by the guanine exchange factor (GEF) eIF2B (Gomez, Mohammad, & Pavitt, 2002). When eIF2 becomes phosphorylated on the  $\alpha$  subunit, its affinity to bind eIF2B is enhanced. Phosphorylated eIF2 $\alpha$  becomes a competitive inhibitor of the GEF. eIF2B concentrations in the cell are much lower than that of eIF2, therefore even slight increases in P-eIF2 $\alpha$  can disrupt the GEF activity of eIF2B (Krishnamoorthy et al., 2001; Pavitt, Ramaiah, Kimball, & Hinnebusch, 1998). During stress conditions when eIF2 $\alpha$  is phosphorylated, the recycling of GDP-eIF2 back to its active form is reduced. The initiation of the TC and 43S PIC are reduced, thereby attenuating the initiation of cap-dependent protein translation (Harding et al., 2000). Despite this halt in global protein translation, there is selective upregulation of the translation of select transcripts, including activating transcription factor 4 (ATF4; Baird & Wek, 2012; Lu, Harding, & Ron, 2004). ATF4 is strongly considered to be the effector of the ISR because it modulates the expression of stress-induced genes.

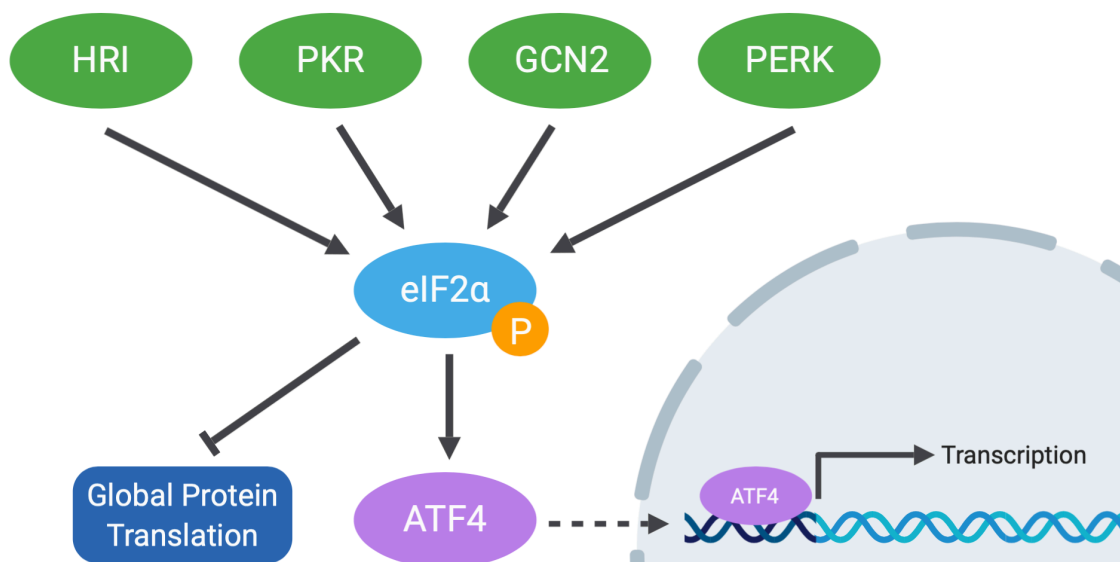


**Figure 1.2. The Integrated Stress Response.** The integrated stress response (ISR) is a conserved intracellular pathway that allows cells to respond to a variety of stressors. HRI, PKR, GCN2, and PERK are the four kinases of the ISR and they each detect specific stressors in the cellular environment. Once a stress stimulus is detected, the corresponding kinase dimerizes and auto-phosphorylates, thereby becoming activated. The kinases converge upon and phosphorylate eIF2 $\alpha$ , resulting in two main consequences: a reduction in global protein translation and a selective increase in translation of a subset of mRNA transcripts. ATF4 protein levels are elevated in response to cellular stress and the transcription factor is able to translocate into the nucleus. Once in the nucleus, ATF4 modulates the expression of downstream target genes involved in processes such as amino acid synthesis, autophagy, and apoptosis.

### 1.2.1 Activating Transcription Factor 4

ATF4 is a member of the activating transcription factor/cyclic AMP response element binding protein (ATF/CREB) family (Karpinski, Morle, Huggenvik, Uhler, & Leiden, 1992; Wortel, van der Meer, Kilberg, & van Leeuwen, 2017). Also known as cAMP-response element binding protein 2 (CREB-2), ATF4 contains a basic leucine zipper (bZIP) domain and is able to homo- or heterodimerize with other bZIP transcription factors (Ameri & Harris, 2008; Karpinski et al., 1992). The three main subfamilies that ATF4 dimerizes with are: ATF/CREB, FOS/JUN, and CCAAT enhancer binding protein (C/EBP) (Vallejo, Ron, Miller, & Habener, 1993; Wortel et al., 2017). The partners that ATF4 interacts with are critical in determining its transcriptional selectivity (Hai & Curran, 1991). ATF4 homodimers are unstable even when bound to DNA, while heterodimers are more stable and bind more readily to DNA targets (Hai, Liu, Coukos, & Green, 1989; Podust, Krezel, & Kim, 2001; Wortel et al., 2017). ATF4 binds to DNA through its basic region upstream of the bZIP domain, which is composed of many positively charged amino acids (Ameri & Harris, 2008; Karpinski et al., 1992). ATF4 heterodimers can bind to various target genes through cAMP responsive elements (CREs) and C/EBP-ATF response elements (CAREs) in the DNA sequence (Baird & Wek, 2012; Hai & Curran, 1991; Vallejo et al., 1993; Wortel et al., 2017). The various transcription factors that ATF4 heterodimerizes with determine the outcome of ISR signaling.

ATF4 protein expression is strictly regulated. It has many functional domains that allow the interaction with and modulation by various factors (Figure 1.3; Dey et al., 2010; Wortel et al., 2017). The N-terminal domain of the protein contains an interaction site for the histone acetyltransferase p300. This interaction stabilizes ATF4 protein by blocking ubiquitination and subsequent proteasomal degradation, however this occurs independently from the acetyltransferase activity of p300 (Ameri & Harris, 2008; Lassot et al., 2005). The half-life of ATF4 protein is approximately 2-4 hours, therefore protein stabilization is important for prolonging its activity (Baird & Wek, 2012; Rutkowski et al., 2006). The oxygen-dependent degradation domain (ODDD) of ATF4 offers another avenue of protein stabilization by interacting with prolyl hydroxylase domain 3 (PHD3), a hypoxia-inducible protein (Köditz et al., 2007; Wortel et al., 2017). Downstream of the

p300 and ODDD interaction domains lies a motif recognized by  $\beta$ -transducin repeats containing protein ( $\beta$ -TrCP).  $\beta$ -TrCP is associated with an E3-ubiquitin ligase (Lassot et al., 2001; Wortel et al., 2017).  $\beta$ -TrCP recognizes nuclear ATF4 phosphorylated on specific sites within the  $\beta$ -TrCP recognition domain and leads to ubiquitination and proteasomal degradation of ATF4 (Lassot et al., 2001). In addition to protein interactions that modulate ATF4 stability, ATF4 is also subject to many post-translational modifications, including phosphorylation, methylation, ubiquitination, and acetylation (Wortel et al., 2017).



The translation of ATF4 is paradoxically enhanced under levels of low global protein translation, when eIF2 $\alpha$  is phosphorylated and the availability of eIF2-GTP-Met-tRNA<sub>i</sub> ternary complexes are low (Harding et al., 2000; Pakos-Zebrucka et al., 2016; Wek, Jiang, & Anthony, 2006). There is still debate within the field, however the primary hypothesis by which phosphorylated eIF2 $\alpha$  preferentially translates *ATF4* is through delayed translation reinitiation and upstream open reading frames (uORFs; Ameri & Harris, 2008; Baird & Wek, 2012; Fernandez, Yaman, Sarnow, Snider, & Hatzoglou, 2002; Harding et al., 2000). uORFs lie 5' to the coding sequence of transcripts.

Translation initiation of ATF4 occurs when the 43S PIC binds to the 5' cap of the transcript and scans until it reaches uORF1. uORF1 is translated and eIF2-GDP disassociates from the mRNA, however the 40S ribosomal subunit continues scanning the transcript. When eIF2-GTP levels are high, under non-stressed conditions, the ternary complex is readily acquired by the small ribosomal subunit and translation is reinitiated at the next start codon on the transcript. This subsequent initiation codon is within uORF2 of the ATF4 mRNA and is inhibitory (Baird & Wek, 2012; Vattem & Wek, 2004). uORF2 overlaps out-of-frame with the coding region of the ATF4 transcript and causes dissociation of the ribosomal complex (Lu et al., 2004; Young & Wek, 2016). When cells are under stressed conditions, eIF2 TC levels are scarce and the 40S ribosomal subunit is unable to acquire a TC in time to reinitiate translation at uORF2. Consequently, the ribosomal subunit bypasses the inhibitory uORF and is able to acquire a ternary complex in sufficient time to recognize the coding region of the *ATF4* transcript (Pitale, Gorbatyuk, & Gorbatyuk, 2017; Vattem & Wek, 2004). Preferential translation of ATF4 during periods of cellular stress results in greater protein expression (Baird & Wek, 2012; Dey et al., 2010).

ATF4 is expressed throughout all cell types and plays an important role in embryonic development (Ameri & Harris, 2008). Studies using murine whole-embryo ATF4 knockouts have revealed that ATF4 plays a critical role in lens formation in the eye, skeletal development, hematopoiesis, lipid metabolism, and fertility, among others (Fischer et al., 2004; Hettmann, Barton, & Leiden, 2000; Masuoka & Townes, 2002; Tanaka et al., 1998; Wang et al., 2010; Yang et al., 2004). Therefore, ATF4 knockout

mice display microphthalmia, stunted growth and low bone mass, and infertility. These developmental abnormalities highlight the importance of ATF4 in normal cell functioning under non-stressed conditions.

When cells are experiencing stress, ATF4, the effector of the integrated stress response, interacts with other transcription factors and modifies the expression of stress-induced genes. These target genes are involved in processes such as amino acid synthesis, autophagy, and protein folding (B'Chir et al., 2013; Harding et al., 2003). The reduction in global protein translation that occurs due to phosphorylation of eIF2 $\alpha$  reduces the energy demands of the cell. This allows the cell to prioritize alleviating the stress it is experiencing. For instance, in response to ER stress, global protein translation is attenuated, thus reducing the load of naïve proteins entering the ER. Consequently, the cell can increase the clearance of unfolded proteins in the ER or increase the expression of ER chaperones (Joshi et al., 2016; Luo, Baumeister, Yang, Abcouwer, & Lee, 2003). The process of autophagy is an important protective pathway that cells utilize to degrade proteins, recycle amino acids, and maintain energy levels. It has been shown that eIF2 $\alpha$  and ATF4 are necessary for the expression of many autophagic genes and ATF4 binds to amino acid response elements (AAREs) in the promoter regions of these genes (B'Chir et al., 2013). In addition, ATF4 binds to and activates the promoter of 78 kDa glucose-related protein, also called binding immunoglobulin protein, (Grp78/BiP), an ER chaperone (Lee, 2001; Luo et al., 2003). This increases the protein folding capacity of the ER. Once cells have adequately dealt with a stressor and returned to homeostasis, they must deactivate the integrated stress response. Dephosphorylation of eIF2 $\alpha$  allows regular protein translation to proceed and is mediated by the protein phosphatase 1 (PP1) complex. It is composed of a catalytic subunit and a regulatory subunit. Growth arrest and DNA damage-inducible protein 34 (Gadd34) is one of the regulatory subunits that can bind with the PP1 catalytic subunit (Ma & Hendershot, 2003). ATF4 induces the expression of Gadd34, which creates a negative feedback loop to deactivate the ISR and restore global protein translation (Novoa et al., 2003; Pakos-Zebrucka et al., 2016).

It is generally accepted that transient activation of the ISR and ATF4 upregulation favour cell survival. In contrast, chronic stress that results in sustained ISR activity and ATF4



protein levels can lead to apoptosis and aberrant cell death (Pitale et al., 2017; Rutkowski et al., 2006; Wortel et al., 2017). One of the most well-characterized ATF4 target genes is C/EBP homologous protein (CHOP), also known as Gadd153. CHOP is a known pro-apoptotic protein and it is also a bZIP transcription factor that can heterodimerize with ATF4 (Fawcett, Martindale, Guyton, Hai, & Holbrook, 1999; Han et al., 2013; Pitale et al., 2017). In response to ER stress, it has been demonstrated that ATF4-CHOP binds to the tribbles-related protein 3 (Trib3) promoter and increases expression, eventually leading to apoptosis (Ohoka, Yoshii, Hattori, Onozaki, & Hayashi, 2005). Additionally, a growing body of evidence suggests that CHOP can also lead to apoptosis through the modulation of the B-cell lymphoma-2 (BCL-2) protein family (Galehdar et al., 2010; Szegezdi et al., 2006; Youle & Strasser, 2008).

The switch from pro-survival to pro-death ISR outcomes is highly context-dependent, and factors such as cell type and the nature or duration of the stress can influence the result (Baird & Wek, 2012; Rutkowski et al., 2006; Wortel et al., 2017). For example, in mouse embryonic fibroblasts (MEFs), the induction of ER stress causes activation of the PERK arm of the ISR and a subsequent increase in ATF4 protein levels (Harding et al., 2003). The researchers found that ATF4-deficient MEFs are more sensitive to oxidative stress and endogenous ATF4 upregulation in wildtype cells helps promote survival. Additionally, high levels of ATF4 protein have been found in hypoxic regions of primary human malignant tumours from breast, skin, and cervical tissues (Bi et al., 2005). Despite pro-survival evidence in some tissues, ATF4 has been shown to favour pro-death outcomes in neurons (Galehdar et al., 2010; Lange et al., 2008). Research suggests that ATF4-deficient neurons are resistant to oxidative and ER stress and subsequent apoptosis.

### 1.2.2 ISR and Apoptosis

The Bcl-2 protein was first discovered in B-cell follicular lymphomas as a pro-survival protein that inhibits cell death when overexpressed (Tsujimoto, Cossman, Jaffe, & Croce, 1985; Vaux, Cory, & Adams, 1988). Bcl-2 is a member of the BCL-2 protein family, which has at least 12 core proteins, as well as numerous proteins that share homology through the BH3 motif (Zha, Aimé-Sempé, Sato, & Reed, 1996). The BCL-2 family

consists of pro-survival, pro-apoptotic, and BH3-only members that interact to determine cell fate. Pro-survival members inhibit cell death by binding to pro-apoptotic members and preventing them from exerting their effects (Willis et al., 2007; Youle & Strasser, 2008). BH3-only proteins promote apoptosis by binding to and sequestering pro-survival members, thus freeing pro-apoptotic proteins (Willis et al., 2007). Apoptosis that occurs through the activation of pro-death BCL-2 members is also referred to as the intrinsic mitochondrial pathway due to the role that mitochondria have in initiating apoptosis. Bcl-2-associated X protein (BAX) and Bcl-2 homologous antagonist killer (BAK) are pro-apoptotic BCL-2 proteins that induce the permeabilization of the outer mitochondrial membrane (OMM) when derepressed (Kuwana et al., 2002). When the OMM is permeabilized, apoptogenic molecules are released into the cytoplasm and cause activation of apoptotic protease-activating factor-1 (APAF1). APAF1 in turn induces activation of caspase-9 and caspase-3, culminating in apoptosis (Li et al., 1997). P53-upregulated modulator of apoptosis (PUMA) is a well-known BH3-only member that is induced in response to p53-dependent and -independent mechanisms and is able to bind to and inhibit all BCL-2 pro-survival members (Cregan et al., 2004; Galehdar et al., 2010; Steckley et al., 2007). Our lab has previously shown that PUMA is upregulated in response to oxidative and ER stressors, and PUMA-deficient neurons are protected against oxidative and ER stress-induced apoptosis (Galehdar et al., 2010; Steckley et al., 2007). In addition, our lab has shown that ATF4-deficient neurons have less PUMA induction and attenuated cell death in response to these stressors (Galehdar et al., 2010). Further studies have determined that CHOP-deficient neurons also have attenuated PUMA expression and apoptosis, and that CHOP-mediated induction of PUMA might occur through the AKT-FOXO3a pathway (Ghosh, Klocke, Ballestas, & Roth, 2012).

## 1.3 The ISR in Alzheimer's disease

### 1.3.1 Cellular stress in AD

The integrated stress response has been implicated in Alzheimer's disease. Specifically, high levels of ISR markers have been found in mouse models of Alzheimer's disease, as well as in humans with AD. Amyloid- $\beta$  can induce high levels of neuronal stress, and the ISR is a way that neurons can try to mitigate cellular stress. In *post mortem* analyses from

AD patients, more ATF4-positive axons were found in the hippocampus and other subcortical structures compared to age-matched controls, and these axons were found surrounding amyloid plaques (Baleriola et al., 2014). Higher levels of phosphorylated eIF2 $\alpha$  have also been found in AD patients' brains compared to healthy controls (Chang, Wong, Ng, & Hugon, 2002; Ma et al., 2013). Additionally, elevations in phosphorylated eIF2 $\alpha$  and ATF4 levels have been measured in APP/PS1 and 5XFAD mouse models of AD (Ma et al., 2013). Cellular stress activates ISR kinases, increases phosphorylated levels of eIF2 $\alpha$ , reduces global protein translation, and facilitates translation of select transcripts. Examples of transcripts that are preferentially translated include ATF4 and BACE1. BACE1, or  $\beta$ -secretase, cleaves amyloid precursor protein through the amyloidogenic pathway, which results in the production of A $\beta$  species of varying lengths. BACE1 is considered to be the rate-limiting enzyme in the production of pathogenic amyloid- $\beta$  (Vassar, Kovacs, Yan, & Wong, 2009). Under basal conditions, the translation of BACE1 is suppressed (Lammich, Schöbel, Zimmer, Lichtenthaler, & Haass, 2004). ATF4 and BACE1 both contain upstream open reading frames in their 5' untranslated regions, which provides one explanation of preferential translation during periods of cellular stress (De Pietri Tonelli et al., 2004; Guix, Sartório, & ILL-Raga, 2019). Elevated levels of phosphorylated eIF2 $\alpha$  and BACE1 expression have been found in the 5XFAD mouse model of Alzheimer's disease (Devi & Ohno, 2014). PERK haploinsufficiency in these mice attenuated high levels of phosphorylated eIF2 $\alpha$  and led to a reduction in BACE1 expression. Additionally, the expression of the A $\beta$ -degrading enzyme neprilysin was reduced. PERK haploinsufficiency in these animals also led to the restoration of NEP expression (Devi & Ohno, 2014). Therefore, PERK dysregulation in the 5XFAD mouse model leads to increased amyloid- $\beta$  production as well as decreased amyloid- $\beta$  clearance. High levels of BACE1 protein and activity levels have also been found in the neocortex in Alzheimer's disease patients (Fukumoto, Cheung, Hyman, & Irizarry, 2002; O'Connor et al., 2008).

Evidence also suggests a link between downstream ATF4 and  $\gamma$ -secretase expression (Mitsuda, Hayakawa, Itoh, Ohta, & Nakagawa, 2007; Ohta et al., 2011).  $\gamma$ -secretase cleaves APP once it has first been cleaved by either  $\alpha$ -secretase or BACE1, generating

amyloid- $\beta$  species of varying lengths. Presenilin-1, which forms the active site of the  $\gamma$ -secretase complex, contains an amino acid response element in its gene promoter. It has been demonstrated that amino acid deprivation activates the ISR kinase GCN2 and leads to phosphorylation of eIF2 $\alpha$  and increased expression of ATF4. Interestingly, it has been found that ATF4 binds to the AARE sequence in the PS1 gene and increases the expression of  $\gamma$ -secretase cofactors in response to amino acid deprivation (Mitsuda et al., 2007).  $\gamma$ -secretase activity is increased in response to ER stress through the expression of ATF4 (Ohta et al., 2011).

In addition to the link between ATF4 and A $\beta$  production, ATF4 has also been shown to induce neurodegeneration in response to amyloid- $\beta$  treatment (Baleriola et al., 2014). Axonally applied A $\beta_{42}$  induced local translation of *Atf4* mRNA, retrograde transport to the soma, and increased expression of ATF4-responsive genes such as CHOP. Prolonged CHOP expression led to apoptosis in these neurons, which was reversed when axonal translation of ATF4 was inhibited (Baleriola et al., 2014). Thus, abundant evidence suggests that ATF4 upregulation seen in Alzheimer's disease may act as both an upstream initiator for pathological amyloid- $\beta$  production and also act downstream of amyloid- $\beta$  as an effector of this stress leading toward neurodegeneration (Wei, Zhu, & Liu, 2015).

### 1.3.2 ISR and Memory

On a cellular level, Alzheimer's disease can be additionally characterized by synaptic dysfunction (Masliah et al., 1994; Nelson et al., 2009). Long-term potentiation (LTP), first characterized in the 1970s in the hippocampus, is a phenomenon that allows for the study of synaptic plasticity (Bliss & Lomo, 1973). The main principle behind LTP is that synaptic connections that are frequently stimulated will be strengthened to facilitate neuronal communication (Bliss & Collingridge, 1993). In experimental settings, LTP is typically induced by applying a short, high-frequency burst of stimulation, called a tetanus, to synapses in a slice of neuronal tissue, most commonly the hippocampus (Bliss & Collingridge, 1993). The tetanic stimulation can induce enhanced synaptic responses as measured by field recordings of excitatory postsynaptic potentials.

Multiple researchers have found that elevations in ISR members are detrimental to long-term potentiation. Costa-Mattioli et al. demonstrated that the genetic removal of GCN2 resulted in a more robust expression of LTP compared to wildtype hippocampal slices. This GCN2 deletion also led to decreased hippocampal ATF4 mRNA translation (Costa-Mattioli et al., 2005). Furthermore, in APP/PS1 mice, PERK removal rescued the spatial memory and synaptic plasticity deficits seen in APP/PS1 mice (Ma et al., 2013). In addition to AD mouse models that contain mutations in APP and PS1 genes, mice expressing the human form of the apolipoprotein E (ApoE)  $\epsilon 4$  allele have also been utilized as models of sporadic Alzheimer's disease (SAD; Segev et al., 2015). ApoE plays a role in lipid metabolism and can promote the clearance of amyloid- $\beta$  in the brain. There are three polymorphic ApoE alleles and having at least one  $\epsilon 4$  allele is associated with a higher risk of developing AD (Strittmatter & Roses, 1997). ApoE  $\epsilon 4$  can induce ER and oxidative stress, leading to high levels of phosphorylated eIF2 $\alpha$  (Segev et al., 2015; Segev, Michaelson, & Rosenblum, 2013). Inhibition of PKR in ApoE  $\epsilon 4$  mice rescued impairments in fear conditioning and reduced hippocampal ATF4 expression to control levels (Segev et al., 2015).

Phosphorylated eIF2 $\alpha$  has been implicated in LTP as well. It has been demonstrated that by blocking the dephosphorylation of eIF2 $\alpha$ , thus increasing the levels of phosphorylated eIF2 $\alpha$ , the initiation of LTP is impeded (Costa-Mattioli et al., 2007). The conversion of early phase to late phase LTP is unable to occur when phosphorylated eIF2 $\alpha$  levels are increased. It has been well-documented that *de novo* protein synthesis is necessary for sustaining LTP (T. Ma et al., 2013). Following tetanic induction of LTP, levels of phosphorylated eIF2 $\alpha$  are physiologically reduced (Trinh et al., 2014). It has been shown that ATF4 can interact with and inhibit CREB, thereby inhibiting the conversion from early to late phase LTP. By inhibiting ATF4, the threshold needed to induce long-term potentiation in mice was lowered and hippocampal-based spatial memory was increased (Chen et al., 2003).

## 1.4 Rationale

ATF4 is part of the stress-responsive ISR pathway and becomes upregulated in response to various cellular stressors. Stimuli such as oxidative and endoplasmic reticulum stressors have been shown to reliably induce the ISR and ATF4 induction. Within the context of Alzheimer's disease, high levels of neuronal stress have been measured. The ISR has been implicated in AD as a mechanism that can exacerbate the effects of amyloid- $\beta$  and also be upstream initiators of synaptic dysfunction and pathological hallmarks (Wei et al., 2015). Previous research has demonstrated that the ISR and ATF4 are induced in animal models of Alzheimer's disease, as well as in the brains of AD patients (Baleriola et al., 2014; Chang et al., 2002; Ma et al., 2013). The knockdown of an ER stress-inducible neurotrophic factor was shown to exacerbate amyloid- $\beta$  toxicity, while overexpression lowered the levels of ER stress and ATF4, partially protecting against neuronal death (Xu et al., 2019). Prolonged ATF4 activation has been shown to induce the expression of pro-apoptotic genes and promote neuronal death. Previous work in our lab has demonstrated that oxidative and ER stress lead to apoptosis in a PUMA-dependent manner (Galehdar et al., 2010). However, it remains unclear whether ATF4-mediated death in response to amyloid- $\beta$  occurs in a PUMA-dependent manner.

## 1.5 Hypothesis

Amyloid- $\beta$ -induced neuronal death occurs through ATF4-mediated upregulation of the pro-apoptotic gene PUMA.

## Chapter 2

### 2 Materials and Methods

#### 2.1 Animals

All animal procedures were performed in accordance with the guidelines set forth by the Animal Care Committee at Western University. Animals were housed in a 12h light-dark cycle and food and water were provided *ad libitum*. Mice with an ATF4-null mutation were obtained from Dr. Tim Townes and Dr. Joe Sun (University of Alabama at Birmingham, AL; Masuoka & Townes, 2002). Mice harboring PUMA-null mutations were generated in the lab of Dr. Andreas Strasser (Walter and Eliza Hall Institute of Medical Research, Bundoora, Victoria, Australia) and obtained from The Jackson Laboratory (C57BL/6-*Bbc3<sup>tm1Ast</sup>/J*, #011067). Both mouse strains were maintained on a C57BL/6 background. Heterozygous animals were bred to generate wildtype and knockout littermates for ATF4 and PUMA strains.

##### 2.1.1 Genotyping

Mouse genomic DNA was isolated by adding DNA lysis buffer (100 mM Tris, 5mM EDTA, 0.2% weight per volume SDS, 200 mM NaCl) and Proteinase K (Bioshop, #PRK222) to embryonic tail clip samples. Samples were incubated overnight in a 55°C heat block. Phenol:Chloroform:Isoamyl alcohol (Fisher Scientific, #BP1752I-400) was added to the samples and tubes were inverted for approximately 1 minute. Tubes were spun for 10 minutes at 12,000 rpm at room temperature. The top aqueous layer was transferred to a clean tube, isopropanol was added, and the tubes were inverted for approximately 30 seconds. Tubes were spun for 10 minutes at 10,000 rpm at 4°C and the supernatant was aspirated. The DNA pellet was washed with 70% ethanol and spun again for 5 minutes at 10,000 rpm at 4°C. The supernatant was discarded, and the pellet was dried at room temperature. The pellet was then dissolved in TE buffer (ThermoFisher, #AM9849) and incubated at 37°C for one hour.

The ATF4 primer sequences used for genotyping are provided in Appendix A. The PCR reaction contained dNTPs, reaction buffer, MgCl<sub>2</sub>, Q solution, Taq polymerase, ddH<sub>2</sub>O, 5

$\mu\text{M}$  of each of the three primers, and 2  $\mu\text{L}$  of DNA. All PCR reagents were purchased from Qiagen (#201207) except for dNTPs, which were purchased from Life Technologies (#10297018). The PCR cycling conditions were as follows: initial activation at 95°C for 2 minutes; denaturation at 94°C for 20 seconds; annealing at 62°C for 30 seconds; elongation at 68°C for 1.5 minutes; final extension at 68°C for 10 minutes; and held at 4°C. The denaturation, annealing, and elongation steps were repeated for 30 cycles prior to the final extension.

PUMA embryos were genotyped using the primer sequences provided in Appendix B. The PCR reaction mix was the same as that used for ATF4 genotyping. The cycling conditions were: initial activation at 94°C for 2 minutes; denaturation at 94°C for 20 seconds; annealing at 60°C for 30 seconds; elongation at 72°C for one minute; final extension at 72°C for 4 minutes; and held at 4°C. The denaturation, annealing, and elongation steps were repeated for 32 cycles prior to the final extension.

## 2.2 Cell culture

### 2.2.1 Primary cortical neurons

Primary cortical neurons were harvested from mice on embryonic day 14.5-15.5 (E14.5-15.5). Pregnant females were injected intraperitoneally with 400  $\mu\text{L}$  euthanyl, at a concentration of 54 mg/mL diluted in 0.9% saline, followed by cervical dislocation. The embryos were removed from the uterus and placed into a petri dish filled with 1 x Hank's Balanced Salt Solution (HBSS; Gibco®, #14170-112) stored on ice. The brains were removed from the embryos, the cortices were isolated, and the meninges were removed. The cortices from each embryo were processed separately. Tail clip samples were also collected from each embryo for genotyping purposes.

Cortices were dissected in calcium- and magnesium-free 1x HBSS and stored in 1x HBSS on ice until ready to process. To dissociate the primary neurons, cortices from individual pups were incubated in 500  $\mu\text{L}$  1x HBSS supplemented with 1x trypsin (Sigma, #T4549) and 1.2 mM  $\text{MgSO}_4$  at 37°C for 25 minutes in a tube rotator. The trypsin solution was inhibited by adding 600  $\mu\text{L}$  of 1x HBSS supplemented with 1.2 mM  $\text{MgSO}_4$ , 0.25 mg/mL DNase I (Worthington, #LS002139), and 0.2 mg/mL trypsin



inhibitor (Roche, #10109878001). The samples were thoroughly mixed and centrifuged at 400 x g for 5 minutes. The supernatant was aspirated, and the tissue pellet was resuspended in 1 mL of 1x HBSS supplemented with 3 mM MgSO<sub>4</sub>, 0.8 mg/mL DNase I, and 1.25 mg/mL trypsin inhibitor. The tissue was then mechanically dissociated by triturating the pellet 10-15 times using a flame-polished pipette. The cell suspension was centrifuged at 400 x g for 5 minutes. The supernatant was removed, and the cell pellet was resuspended in 2 mL of cortical neuron medium, composed of Neurobasal Plus medium (NBM; ThermoFisher, #A35829-01) supplemented with 1x B27 plus (ThermoFisher, #A35828-01), 0.5x Glutamax (ThermoFisher, #35050-061), and 50 U/mL penicillin: 50 µg/mL streptomycin (PenStrep; ThermoFisher, #15140-122).

The cell suspensions were then diluted in cortical neuron media to a density of 6x10<sup>5</sup> cells/mL and plated in 35 mm (2 mL; 1.2x10<sup>6</sup> cells/dish) or 4-well (500 µL; 3x10<sup>5</sup> cells/well) dishes. The NunclonΔ surface cell culture dishes (ThermoScientific, #150318, #176740) were coated overnight prior to use with poly-L-ornithine (Sigma, #P4957) diluted 1:10 in ddH<sub>2</sub>O (Invitrogen, #10977023) and incubated at room temperature. Prior to plating the cortical neurons, the dishes were rinsed using ddH<sub>2</sub>O and left to dry completely. Cultures were kept in an incubator at 37°C and 5% CO<sub>2</sub> until used for experiments. Cultured neurons were used following 5-7 days *in vitro* (5-7 DIV).

## 2.2.2 Drugs

The following protocol was used to resuspend amyloid-β<sub>1-42</sub> lyophilized peptide (rPeptide, #A-1001-2) and amyloid-β<sub>1-42</sub> scrambled lyophilized peptide (rPeptide, #A-1004-2). The lyophilized peptides were equilibrated at room temperature 30 minutes prior to processing. Amyloid-β peptide was resuspended in 1 mL 1,1,1,3,3,3-Hexafluoro-2-Propanol (HFIP; Aldrich, #105228-5G) at 1 mg/mL, vortexed, and quickly aliquoted equally into two tubes and sealed. The tubes were then incubated at room temperature for 2 hours to allow for monomerization of the peptide. The vials were then opened and concentrated under vacuum using a SpeedVac® centrifuge (ThermoSavant, #ISS110). The amyloid-β peptide films were sealed and stored at -80°C until further use. One amyloid-β film, 500 µg, was resuspended in 115 µL dimethylsulfoxide (DMSO; Sigma,

#D2650) to obtain a concentration of 1 mM A $\beta$ . A $\beta$ /DMSO was sonicated in a Branson 3510 water bath for 10 minutes and then divided into 5  $\mu$ L aliquots. Resuspended aliquots of amyloid- $\beta$  were stored at -20°C until needed.

A single A $\beta$ <sub>1-42</sub> peptide is approximately 4.5 kDa in size, therefore, dimers and higher order oligomers should be between 10 kDa and 25 kDa. To ensure the A $\beta$  peptide film had been properly resuspended, aliquots were used to check the size of the peptide. Each aliquot was incubated with 15  $\mu$ L PBS overnight at 4°C to allow for oligomerization. An equal volume of non-reducing loading dye was added, and the samples were run on a 15% sodium dodecyl sulfate polyacrylamide gel (SDS-PAGE) at fixed 90V. Once the samples had run down most of the gel, the gel was stained with Imperial™ Protein Stain (ThermoScientific, #24615) for 1h at room temperature and rinsed overnight with milliQ water (Figure 2.1).

Prior to treatments, 1 mM aliquots of A $\beta$ <sub>1-42</sub> and A $\beta$ <sub>1-42</sub> scrambled peptide were diluted in conditioned cortical neuron medium to achieve a final concentration of 1  $\mu$ M when added to the cultures. A concentration of 1  $\mu$ M was used for all treatments with A $\beta$ <sub>1-42</sub> and A $\beta$ <sub>1-42</sub> scrambled. This concentration was chosen based on a dose response experiment, where 1  $\mu$ M was the lowest concentration that reliably induced neuronal stress and ATF4 expression.

Thapsigargin (TG; Sigma, #T9033) is an endoplasmic-reticulum stressor and was used as a positive control to ensure the ISR was being induced. A 1 mM stock solution was made by solubilizing TG in DMSO. All treatments were diluted in conditioned cortical neuron medium and a final concentration of 1  $\mu$ M was achieved when added to the neuronal cultures.

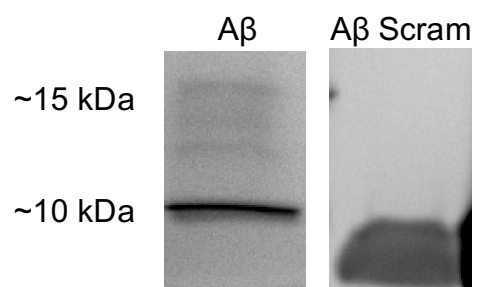


**Figure 2.1. Oligomeric and scrambled amyloid- $\beta$  peptides.** Amyloid- $\beta$  and scrambled amyloid- $\beta$  peptide were resuspended and run on an SDS-PAGE gel. Gels were stained to visualize the size of the peptides.

## 2.3 Protein extraction and quantification

Following appropriate treatment times, cells were rinsed with 1 x phosphate buffered saline (PBS) and then lysed directly in the cell culture dishes using RIPA buffer (Sigma, #R0278) supplemented with 1:100 phosphatase inhibitor cocktail (Sigma, #P5726) and 1:100 protease inhibitor cocktail (Sigma, #P8340). Cells were scraped and transferred into 1.5 mL microcentrifuge tubes. Tubes were placed on ice for a minimum of 30 minutes. Samples were centrifuged at 12,000 x g for 15 minutes at 4°C. The supernatant was transferred to a fresh, labeled tube and samples were stored at -80°C until further use.

To determine the protein concentration of the samples, the Pierce™ BCA Protein Assay Kit (ThermoScientific, #23225) was performed according to the user guide. Using a SpectraMax M5 multi-mode microplate reader (Molecular Devices), absorbance of the samples was measured at 562 nm. The absorbance values of a standard curve were used to calculate the concentrations of protein samples.

## 2.4 RNA isolation and quantification

TRIzol™ reagent (Invitrogen, #15596026) was used to isolated RNA from cultured neurons. The manufacturer's protocol was followed. RNA concentrations of samples were measured using a NanoDrop1000 Spectrophotometer (ThermoScientific). Samples were diluted to 10 ng/μL in ddH<sub>2</sub>O stored at -80°C until used.

## 2.5 Western blot analysis

Protein extracts were separated using 12% SDS-PAGE run at constant 30 mA. Protein gels were then transferred to Immun-Blot® PVDF membranes (BioRad, #1620177) and blocked in 5% milk diluted in 1 x TBST. Membranes were probed with primary antibodies, diluted 1:1000 in blocking solution, targeting ATF4 (Abcam, #184909) and cyclophilin β (Abcam, #178397) overnight at 4°C. Cyclophilin β was used as a loading control. Membranes were then rinsed with 1 x TBST and probed with horseradish peroxidase secondary antibody conjugate (BioRad, #1706515) diluted 1:10,000 in blocking solution for 1h at room temperature. Clarity Western ECL Substrate (BioRad, #1705061) was used to visualize immunoreactive bands. Western blots were first

quantified by normalizing ATF4 levels to Cyclophilin  $\beta$  levels for each sample across experiments. A mean normalized ATF4 value was generated from control-treated samples. This mean value was used to re-normalize all treatments and generate a fold change in ATF4 protein levels relative to control.

## 2.6 Real-time quantitative RT-PCR analysis

Reverse transcription PCR analysis was performed using the Quantifast RT PCR Kit (Qiagen, #204154). Primer sequences targeting CHOP, Trib3, Gadd45 $\alpha$ , 4eBP1, PUMA, and S12 are provided in Appendix C. The reaction setup and cycling protocol were administered according to manufacturer guidelines. Each real-time PCR reaction had a total volume of 25  $\mu$ L which included 40 ng of RNA and forward and reverse primers at a concentration of 1  $\mu$ M. A CFX Connect<sup>TM</sup> Real Time System (Biorad, Mississauga, Canada) was used. The cycling conditions were as follows: reverse transcription for 10 minutes at 50°C, initial PCR activation for 5 minutes at 95°C, and two-step cycling which consisted of denaturation for 10 seconds at 95°C and then combined annealing and extension for 30 seconds at 60°C. The two-step cycling was repeated for a total of 40 cycles. A melting curve analysis was performed at the end to ensure primer specificity.

Changes in gene expression were determined using the  $\Delta(\Delta C_t)$  method.  $\Delta C_t$  values were generated for each sample by normalizing the  $C_t$  value of a gene of interest to the  $C_t$  value of the housekeeping gene S12. The  $\Delta C_t$  values for control treatments were averaged to generate a mean control  $\Delta C_t$  value. The  $\Delta C_t$  for all samples was then normalized to this mean control  $\Delta C_t$ , generating a  $\Delta(\Delta C_t)$  value. Fold changes in gene expression were calculated by using the equation  $2^{-\Delta(\Delta C_t)}$ . For knockout and wildtype PCR data,  $\Delta(\Delta C_t)$  values were calculated by normalizing all samples to the mean  $\Delta C_t$  value of wildtype controls.

## 2.7 Cell death assay

Cell death assays were performed using the nuclear stain Hoechst 33342 (10  $\mu$ g/mL; Invitrogen, #H1399). Following appropriate treatment times, cells plated in 4-well dishes were fixed with 4% PFA for 30 minutes and then washed with 1 x PBS 3 times. The

second wash included Hoechst 33342 diluted 1:1000 in 1 x PBS. The stain was incubated for 10 minutes at room temperature in the dark. Fixed and stained cells were stored in 1 x PBS. Images of the cells were captured at 20x magnification on an Olympus IX70 microscope. A CCD camera (Q-imaging, Burnaby, BC, Canada) and Northern Eclipse software (Empix imaging, Mississauga, ON, Canada) were used to capture images. Five separate fields were captured per well. Images were counted using ImageJ software with Fiji plugins (ImageJ, National Institutes of Health, Maryland, USA). Apoptotic nuclei as well as total nuclei were counted for each image and counts were averaged per well. Nuclei were manually counted based on their morphology. Live cells show a diffuse pattern of staining, while apoptotic cells have condensed, bright, and sometimes fragmented patterns of staining. Percent apoptotic nuclei were calculated for each well and counts for each treatment were averaged.

## 2.8 Caspase-3 activity assay

Caspase activity assays were performed using protein samples extracted in caspase lysis buffer. The lysis buffer stock contained 10 mM Hepes (Fisher Bioreagents, #BP299-500), 1 mM KCl, 1.5 mM MgCl<sub>2</sub>, and 10% glycerol diluted in ddH<sub>2</sub>O. The following reagents were added fresh before use: 5 µg/mL Apropin+, 2 µM/mL Leupeptin, 0.2 mg/mL PMSF, 0.1% NP40, and 1 µM DTT. Treated cells had their media aspirated and were washed with 1 x PBS before adding caspase cell lysis buffer directly to the dishes. Cells were scraped and transferred to 1.5 mL microcentrifuge tubes and incubated on ice for 30 minutes. Lysates were centrifuged at 12,000 x g for 15 minutes at 4°C. The supernatant was collected and transferred to a fresh, labelled tube. Protein samples were stored at -80°C. Protein concentration was determined by BCA assay as described above.

Caspase-3 activity was measured using fluorescence generated by the cleavage of the substrate Ac-DEVD-AFC (Biomol, #P-409). Caspase activity buffer was composed of ddH<sub>2</sub>O supplemented with 25 mM Hepes, 10 mM DTT, 10% sucrose, 0.1% CHAPS (Roche, #10810118001), and 15 µM Ac-DEVD-AFC. Activity buffer was added to an opaque 96-well plate along with 0.5 µg of caspase protein per well, plated in duplicates. Fluorescence was measured every 20 minutes for 2 hours on a SpectraMax M5 multi-mode microplate reader (Molecular Devices), with excitation 400 nm and emission 505

nm. Fluorescence was measured in arbitrary fluorescence units (AFU). Fold change in caspase activity was calculated by normalizing AFU values across treatments and genotypes to the mean AFU of wildtype controls.

## 2.9 Fluorescent immunocytochemistry

Following appropriate treatment times, primary cortical neurons plated on 12 mm glass cover slips (VWR, #48366-251) in 4-well dishes were fixed with 4% PFA for 30 minutes. Cells were permeabilized with ice-cold methanol for 5 minutes, and then washed for 5 with 1 x PBS three separate times. Blocking in 2% BSA in 1 x PBS was performed for one hour at room temperature. The cells were then incubated with primary antibody targeting cytochrome C (Invitrogen, #338200) diluted 1:200 in blocking solution overnight at 4°C. The next day, cells were washed with 1 x PBS three times and were incubated with AlexaFluor® 488 wavelength secondary antibody (Invitrogen, #A11059) diluted 1:500 in blocking solution for 2 hours at room temperature. The cells were washed with 1 x PBS and stained with Hoechst 33342 diluted 1:1000 in 1 x PBS for 10 minutes. The coverslips were mounted onto glass microscope slides (VWR, #48311-600) using ProLong™ Gold mounting glue (Invitrogen, #P36930). Images were taken using the EVOS Imaging System (ThermoFisher). ImageJ with Fiji plugins (ImageJ, National Institutes of Health, Maryland, USA) was used to quantify images and determine the amount of cytochrome C-positive cells in each field, expressed as a percentage of total cells. Images were manually counted for neurons showing retained cytochrome C signal.

## 2.10 Data analysis

Data are reported as mean  $\pm$  standard error of the mean (SEM). Statistical analyses performed were ordinary one-way and two-way ANOVA with Tukey and Sidak post-hoc tests. GraphPad Prism version 8.2.0 for Mac (GraphPad Software, La Jolla, California, USA) was used to perform statistical testing. Statistical significance was set as  $p < .05$ .

## Chapter 3

### 3 Results

ATF4 protein is increased in response to various cellular stressors, including endoplasmic reticulum stress. Thapsigargin (TG) was used to reliably induce ER stress and the ISR, leading to increases in endogenous ATF4 levels. TG increases cytosolic calcium concentrations by inhibiting calcium ATPase pumps and leads to ER stress (Lytton, Westlin, & Hanley, 1991). Previously, our lab has shown that TG treatment induces large increases in ATF4 protein levels and leads to apoptosis in an ATF4-dependent manner (Galehdar et al., 2010). Therefore, TG was used as a reliable inducer of the ISR and ATF4 protein in this study.

#### 3.1 Amyloid- $\beta$ activates the ISR *in vitro*

Firstly, we wanted to confirm that our preparation of oligomeric amyloid- $\beta$  activated the integrated stress response and increased ATF4 protein levels *in vitro*. Neurons were treated for 6, 12, or 24 hours with 1  $\mu$ M amyloid- $\beta$ , 12 hours with 1  $\mu$ M TG, or untreated (UT). Following appropriate treatment times, protein was isolated, processed, and run on an SDS polyacrylamide gel (Figure 3.1A). Once imaged, densitometric measurements were taken and protein bands were normalized to calculate changes in ATF4 protein expression relative to controls (Figure 3.1B). ATF4 protein was increased more than six-fold following 6 hours of A $\beta$ , 12 hours of A $\beta$ , and 12 hours of TG (\*  $p < .05$ ; \*\*  $p < .01$ ;  $n \geq 4$ ). Initially, ATF4 might be activated in an effort to mitigate neuronal stress, however prolonged activation may exacerbate the stress (Pitale et al., 2017). We can conclude that amyloid- $\beta$  treatment does activate the ISR and result in a sustained increase in ATF4 protein levels.



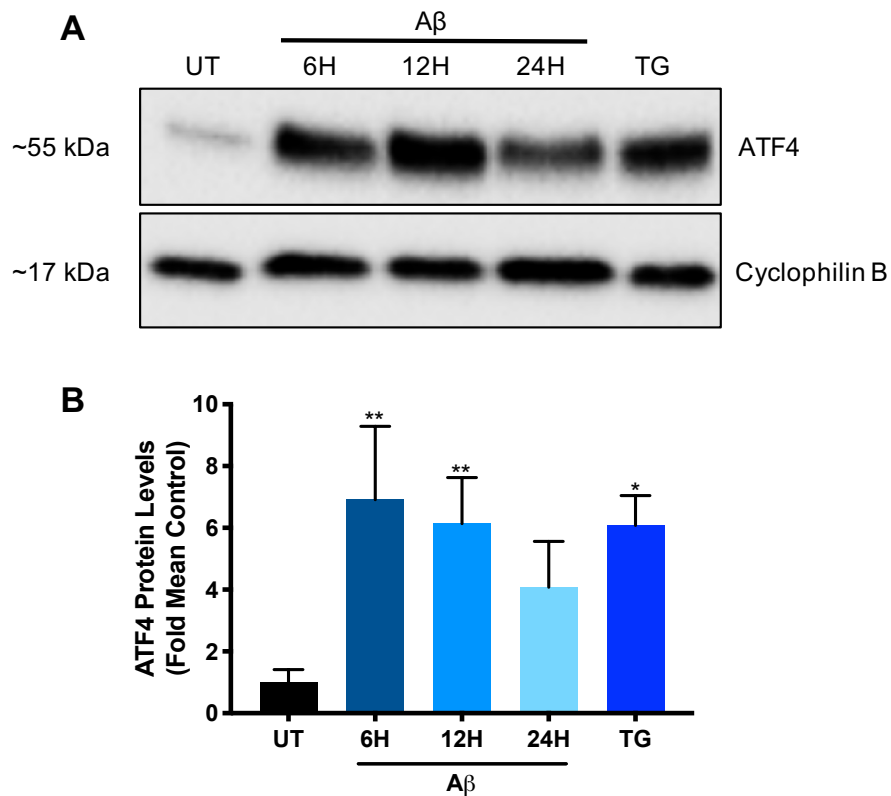


**Figure 3.1. Oligomeric amyloid- $\beta$  induces ATF4 expression.** Primary cortical neurons were treated with oligomeric amyloid- $\beta$  for 6, 12, or 24 hours, 1  $\mu$ M thapsigargin for 12 hours, or left untreated. Protein was then extracted and run on SDS-PAGE gels and probed for ATF4 protein. A) a representative blot of amyloid- $\beta$ -induced ATF4 expression. B) Densitometric measurements were taken and data is presented as mean  $\pm$  SEM of ATF4 fold change relative to control ( $n \geq 4$ ). A one-way ordinary ANOVA and Sidak multiple comparisons tests demonstrated a significant increase in ATF4 protein expression following 6 and 12 hours of amyloid- $\beta$  and 12 hours of thapsigargin (\*  $p < .05$ ; \*\*  $p < .01$ ).

## 3.2 Amyloid- $\beta$ increases pro-apoptotic gene expression

Next, we wanted to investigate if the amyloid- $\beta$ -induced increase in ATF4 expression resulted in increased ATF4 activity. ATF4 can modulate the expression of many target genes through its activity as a transcription factor (Baird & Wek, 2012; Wortel et al., 2017). To study ATF4 transcriptional activity, we chose four mRNA transcripts that have been suggested to favour pro-apoptotic cellular outcomes: CHOP, Trib3, Gadd45 $\alpha$ , and 4eBP1. Previously, it has been shown that CHOP is induced following ER stress and leads to apoptosis through the BCL-2 protein family (Galehdar et al., 2010). Ohoka et al. demonstrated that ATF4 and CHOP activate the Trib3 promoter and Trib3 leads to ER stress-induced apoptosis (Ohoka et al., 2005). Growth arrest and DNA damage-inducible protein 45 $\alpha$  (GADD45 $\alpha$ ) has been shown to be elevated in response to excitotoxicity in a mouse hippocampal cell line, as well as play a role in mitochondrial-dependent apoptosis by interacting with BCL-2 family members (Choi, Kang, Fukui, & Zhu, 2011; Tong et al., 2005). Eukaryotic initiation factor 4E-binding protein 1 (4eBP1) binds to and inhibits eIF4E, a second regulatory hub for the initiation of cap-dependent protein translation (Beugnet, Wang, & Proud, 2003; Gingras, Raught, & Sonenberg, 2002; Hay & Sonenberg, 2004; X. M. Ma & Blenis, 2009). Lastly, a microarray previously performed in our lab demonstrated the upregulation of these transcripts in response to ER stress (Cregan Lab, unpublished). Taken together, these transcripts have been shown to be involved in apoptosis and protein translation, therefore we wanted to further investigate the expression of these transcripts following amyloid- $\beta$  treatment.

Primary cortical neurons were treated with 1  $\mu$ M amyloid- $\beta$  for 6 hours, 12 hours, or 24 hours, 1  $\mu$ M TG for 12 hours, or untreated. Once RNA was isolated, quantitative real-time PCR (qRT-PCR) was performed. Data are reported as fold change relative to untreated controls ( $n \geq 5$ ). CHOP expression was increased more than three-fold following all treatments with amyloid- $\beta$  and close to six-fold following TG treatment (Figure 3.2A). Expression of Trib3 (Figure 3.2B) and Gadd45 (Figure 3.2C) were induced more than 3-fold following A $\beta$  treatment for 12 and 24 hours, and more than 4-fold following treatment with TG. 4eBP1 expression was significantly increased more than 4-fold following 12 hours of A $\beta$  and TG treatments (Figure 3.2D). Oligomeric

amyloid- $\beta$  therefore induces the sustained expression of pro-apoptotic genes (\*  $p < .05$ ; \*\*  $p < .01$ ; \*\*\*  $p < .001$ ; \*\*\*\*  $p < .0001$ ).

### 3.3 Amyloid- $\beta$ induces neuronal apoptosis

As mentioned earlier, prolonged activation of the ISR, and prolonged elevations in ATF4 levels can lead to apoptosis (Galehdar et al., 2010; Lange et al., 2008). Following 24 hours and 48 hours of amyloid- $\beta$  treatment, a nucleic stain was performed to examine whether our AD-like paradigm culminated in neuronal apoptosis (Figure 3.3A). Control and amyloid- $\beta$ -treated neurons were fixed and stained using a Hoechst stain ( $n = 5$ ). A significant increase in apoptotic nuclei following 24 hours ( $41.7\% \pm 2.7$ ) and 48 hours ( $63.5\% \pm 1.8$ ) of A $\beta$  treatment was found, compared to control levels at 48h ( $26.1\% \pm 5.6$ ; \*  $p < .05$ ; \*\*\*\*  $p < .0001$ ). Additionally, there is a significant increase in apoptosis between 24 hours and 48 hours of amyloid- $\beta$  treatment (\*\* $p < .01$ ). Neuronal apoptosis was greatest following 48 hours of amyloid- $\beta$  treatment (Figure 3.3B). Therefore, oligomeric A $\beta$  increased ATF4 protein levels, increased the expression of pro-apoptotic transcripts, and induced apoptotic cell death.

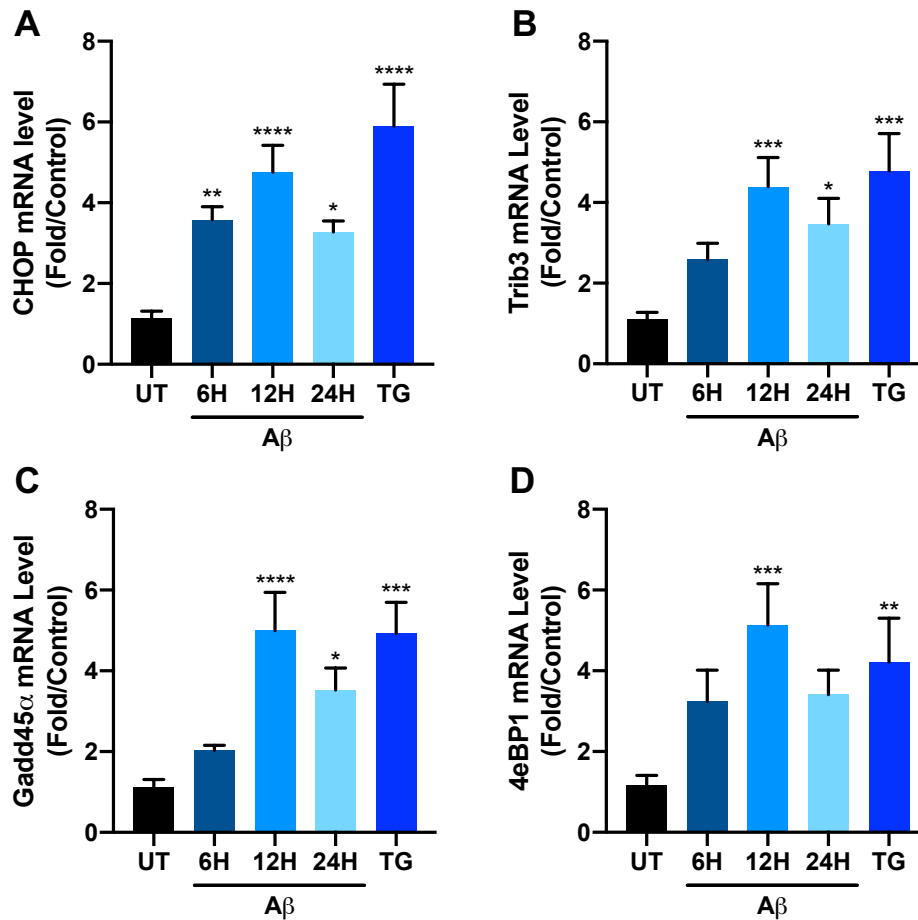


**Figure 3.2. Amyloid- $\beta$  induces pro-apoptotic gene expression.** Primary cortical neurons were treated with 1  $\mu$ M oligomeric amyloid- $\beta$  for 6, 12, or 24 hours, 1  $\mu$ M TG for 12 hours or left untreated. RNA was isolated and probed for multiple reported pro-apoptotic genes using qRT-PCR. Genes probed were: A) CHOP, B) Trib3, C) Gadd45 $\alpha$ , and D) 4eBP1. Amyloid- $\beta$  and TG-treated neurons showed robust increases in apoptotic gene expression as analyzed by one-way ordinary ANOVA and Sidak post-hoc tests (\*  $p < .05$ ; \*\*  $p < .01$ ; \*\*\*  $p < .001$ ; \*\*\*\*  $p < .0001$ ). Data shown are mean  $\pm$  SEM of mRNA fold changes relative to untreated controls ( $n \geq 5$ ).

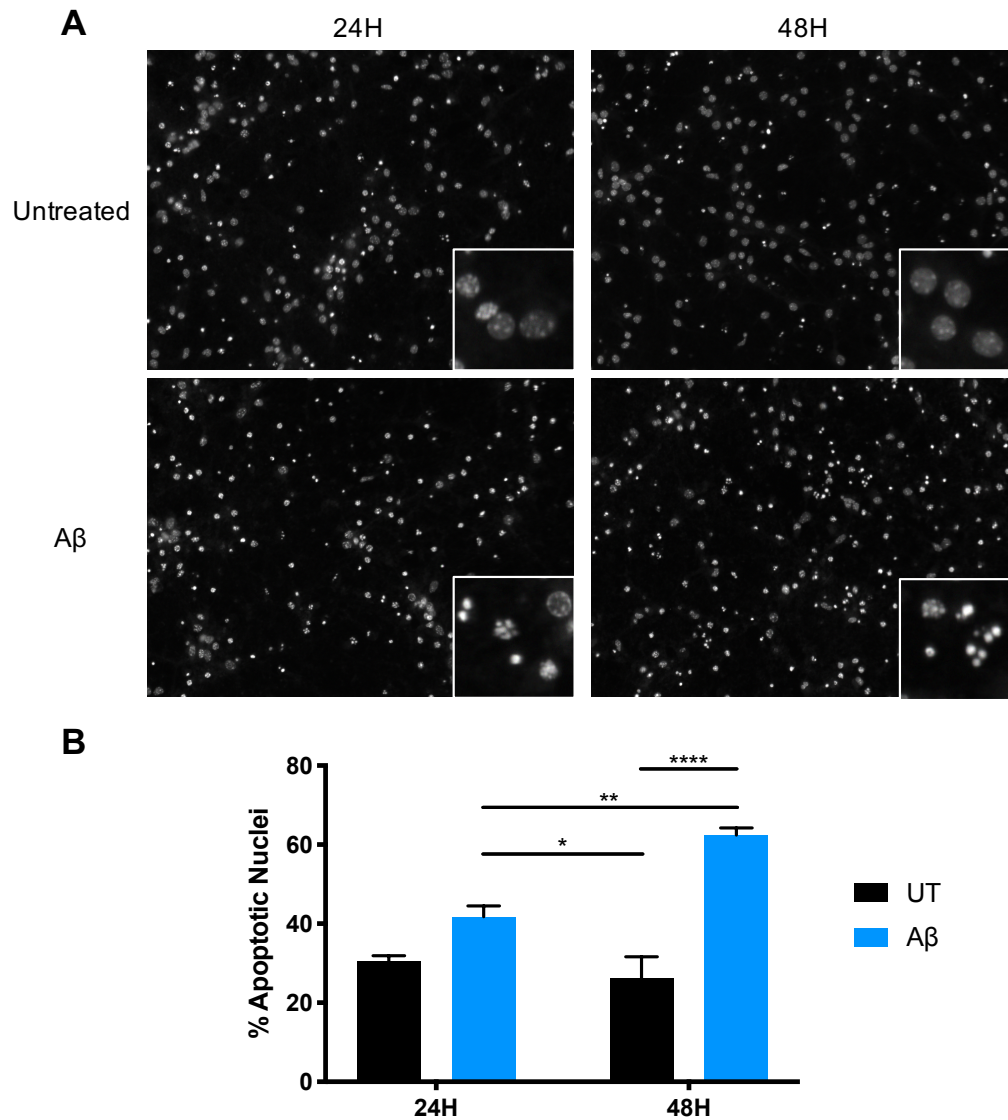


**Figure 3.3. Oligomeric amyloid- $\beta$  induces neuronal apoptosis.** Primary cortical neurons were treated with or without 1  $\mu$ M A $\beta$  for 24 and 48 hours prior to fixation and nuclear Hoechst staining. A) Representative images showing nuclear morphology following 24 or 48 hours of amyloid- $\beta$  or control treatments. B) Apoptotic and total nuclei per treatment were counted and expressed as a percentage. Data shown are mean  $\pm$  SEM of the percentage of apoptotic nuclei (n = 5). A two-way ordinary ANOVA and Tukey post-hoc tests revealed a significant increase in apoptotic following 24 hours and 48 hours of amyloid- $\beta$  treatment (\* p < .05; \*\*\*\* p < .0001). Apoptosis was also significantly increased between 24 and 48 hours of A $\beta$  treatment (\*\* p < .01).

### 3.3.1 Amyloid- $\beta$ -induced toxicity is sequence specific

In order to confirm that amyloid- $\beta$ -induced toxicity is specific to its amino acid sequence, we utilized a scrambled peptide sequence of A $\beta$ . We probed for changes in ATF4 protein levels and apoptotic cell death. Treatment with 1  $\mu$ M A $\beta$  scrambled peptide for 12 hours did not increase ATF4 protein levels compared to controls (Figure 3.4A;  $p > .05$ ;  $n = 5$ ). Treatment with 1  $\mu$ M oligomeric amyloid- $\beta$  for 12 hours induced a significant increase in ATF4 protein expression compared to both untreated and scrambled A $\beta$  treatments ( $* p < .05$ ; Figure 3.4B). A Hoechst stain was performed 48 hours-post treatments with control, 1  $\mu$ M A $\beta$  scrambled peptide, and 1  $\mu$ M A $\beta$  ( $n = 3$ ; Figure 3.4C). Apoptosis was increased following A $\beta$  treatment ( $66.2\% \pm 12$ ) compared to both UT ( $32.9\% \pm 6.4$ ) and scrambled A $\beta$  ( $34.3\% \pm 7.1$ ;  $* p < .05$ ; Figure 3.4D). There was no significant difference in cell death between UT and scrambled A $\beta$  groups ( $p > .05$ ). Therefore, we concluded that amyloid- $\beta$ -induced toxicity is specific to its amino acid sequence.

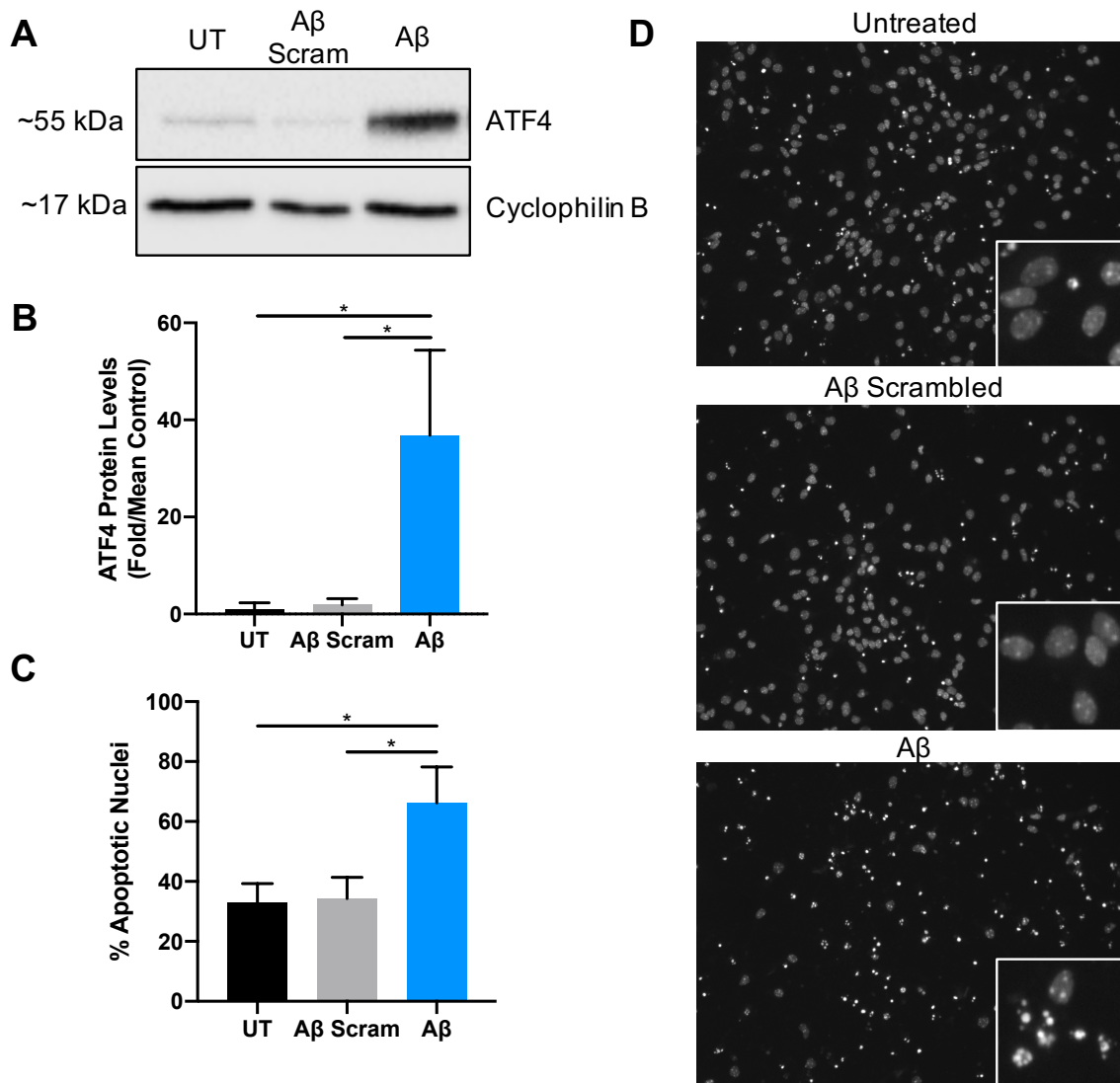


**Figure 3.4. Scrambled amyloid- $\beta$  does not induce cellular stress.** Primary cortical neurons were treated with 1  $\mu$ M A $\beta$ , 1  $\mu$ M A $\beta$  Scram or control-treated for 12 hours prior to protein analysis. A) Protein lysates were separated on SDS-PAGE gels and probed for ATF4. B) Scrambled amyloid- $\beta$ -treated neurons showed no difference in ATF4 protein expression compared to untreated controls ( $p > .05$ ). A $\beta$ -treated neurons showed significant induction of ATF4 compared to both untreated and scramble-treated neurons ( $* p < .05$ ). An ordinary one-way ANOVA with Sidak multiple comparisons was performed to determine any differences in ATF4 expression between groups. Data reported are mean  $\pm$  SEM of fold changes in ATF4 expression relative to control ( $n = 5$ ).

C) Representative Hoechst stain images of untreated, A $\beta$  scram-treated, and A $\beta$ -treated neurons treated for 48 hours. D) Apoptotic nuclei are expressed as a percentage and presented as mean  $\pm$  SEM (n = 3). An ordinary one-way ANOVA and Sidak post-hoc tests revealed a significant increase in apoptotic death following 48 hours of A $\beta$  treatment compared to untreated and A $\beta$  scrambled-treated neurons (\* p < .05). There were no significant differences in apoptotic death between UT and A $\beta$  Scram neurons.



### 3.4 ATF4-deficiency attenuates pro-apoptotic gene expression

Since amyloid- $\beta$  treatment induced the expression of ATF4 protein and pro-apoptotic genes, culminating in apoptosis, we next investigated if deleting ATF4 from these neurons protects against A $\beta$ -induced toxicity. ATF4 heterozygous (ATF4<sup>+/-</sup>) mice were bred to generate ATF4 wildtype (ATF4<sup>+/+</sup>; WT) and ATF4 knockout (ATF4<sup>-/-</sup>; KO) littermates. ATF4<sup>+/+</sup> (n = 9) and ATF4<sup>-/-</sup> (n = 5) cortical neurons were treated with and without 1  $\mu$ M amyloid- $\beta$  for 12 hours and RNA was isolated. We probed for changes in the mRNA expression of CHOP, Trib3, Gadd45 $\alpha$ , and 4eBP1 through qRT-PCR. A $\beta$ -treated wildtype neurons showed an eleven-fold increase in CHOP expression (Figure 3.5A), a fourteen-fold increase in Trib3 expression (Figure 3.5B), and an eight-fold increase in both Gadd45 $\alpha$  (Figure 3.5C) and 4eBP1 expression (Figure 3.5D) compared to untreated wildtype controls (\*\* p < .01; \*\*\*\* p < .0001). In A $\beta$ -treated ATF4 knockout neurons, pro-apoptotic gene expression was attenuated (\*\* p < .01; \*\*\* p < .001; \*\*\*\* p < .0001). No significant difference between untreated ATF4<sup>+/+</sup> and untreated ATF4<sup>-/-</sup> groups were found for all four genes probed (p > .05). There was also no statistical difference between untreated WT and untreated KO neurons compared to A $\beta$ -treated knockout neurons (p > .05). The attenuation of pro-apoptotic gene expression in knockout neurons treated with amyloid- $\beta$  demonstrates the responsiveness of these transcripts to the presence of ATF4.

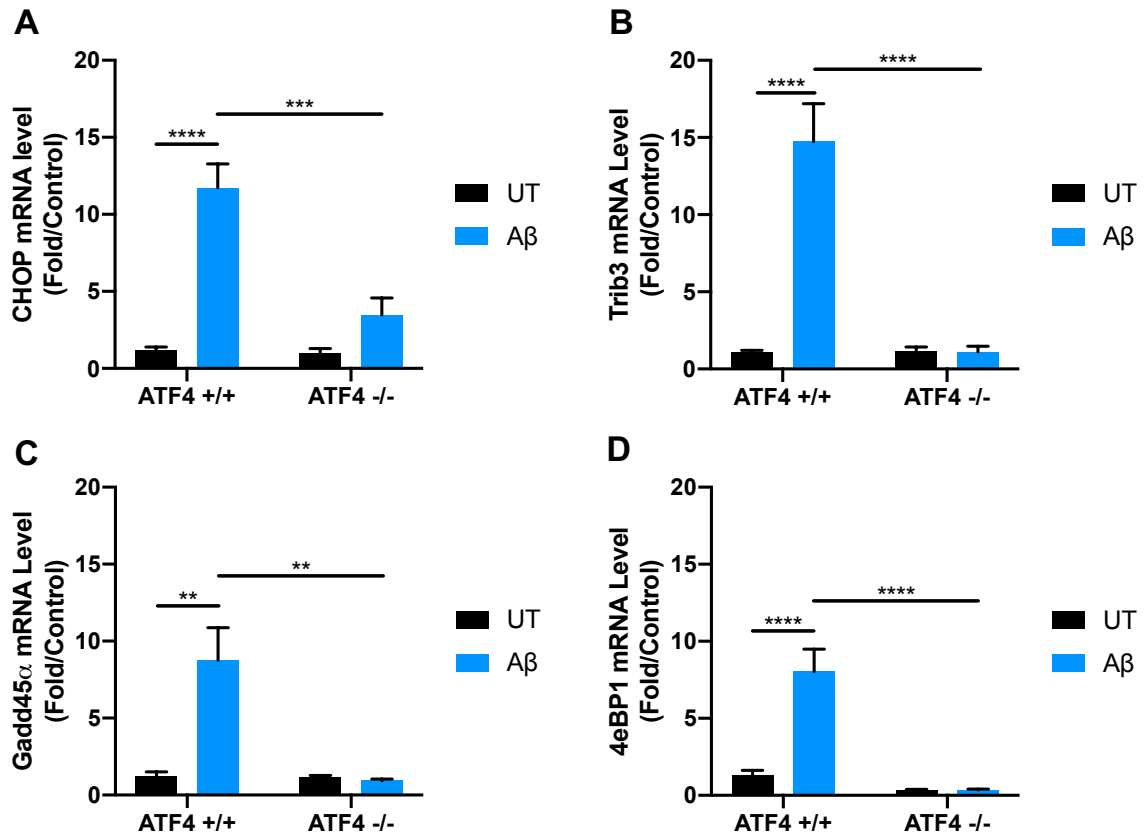


**Figure 3.5. Pro-apoptotic gene expression is attenuated in ATF4-deficient neurons.**

ATF4 wildtype and knockout neurons were treated with and without 1  $\mu$ M amyloid- $\beta$  for 12 hours prior to RNA isolation. qRT-PCR was performed probing for the following genes: A) CHOP, B) Trib3, C) Gadd45 $\alpha$ , and D) 4eBP1. Amyloid- $\beta$  robustly induced the expression of all four pro-apoptotic genes in ATF4<sup>+/+</sup> neurons, which was attenuated in A $\beta$ -treated ATF4<sup>-/-</sup> neurons (\*\*  $p < .01$ ; \*\*\*  $p < .001$ ; \*\*\*\*  $p < .0001$ ). An ordinary two-way ANOVA and Tukey post-hoc tests were performed to determine statistical significance. Data are reported as mean  $\pm$  SEM of mRNA fold changes relative to untreated wildtype controls (ATF4<sup>+/+</sup>  $n = 9$ ; ATF4<sup>-/-</sup>  $n = 5$ ).

### 3.5 Apoptosis is attenuated in ATF4-deficient neurons

We next investigated apoptotic death in ATF4 wildtype and knockout neurons following control and amyloid- $\beta$  treatments. A Hoechst stain was used to identify apoptotic nuclei following 24 hours and 48 hours of treatment (Figure 3.6A; ATF4<sup>+/+</sup> n = 7; ATF4<sup>-/-</sup> n = 6). Cell death was significantly increased in ATF4<sup>+/+</sup> neurons treated with amyloid- $\beta$  (42.5%  $\pm$  4.8) for 24h compared to ATF4<sup>+/+</sup> controls (21.3%  $\pm$  1.5; \*\*\* p < .001).

Apoptosis was attenuated in ATF4 knockout neurons treated with A $\beta$  for 24h (23.2%  $\pm$  2.0; \*\* p < .01; Figure 3.6B). The same pattern was observed in neurons treated for 48h, with the increase in cell death even greater in ATF4<sup>+/+</sup> neurons treated with A $\beta$  (65.6%  $\pm$  3.2; \*\*\*\* p < .0001; Figure 3.6C). Neuronal apoptosis in ATF4 knockout neurons treated with amyloid- $\beta$  was attenuated to control levels regardless of the length of treatment (p > .05). Therefore, ATF4 is necessary for amyloid- $\beta$ -induced apoptosis.

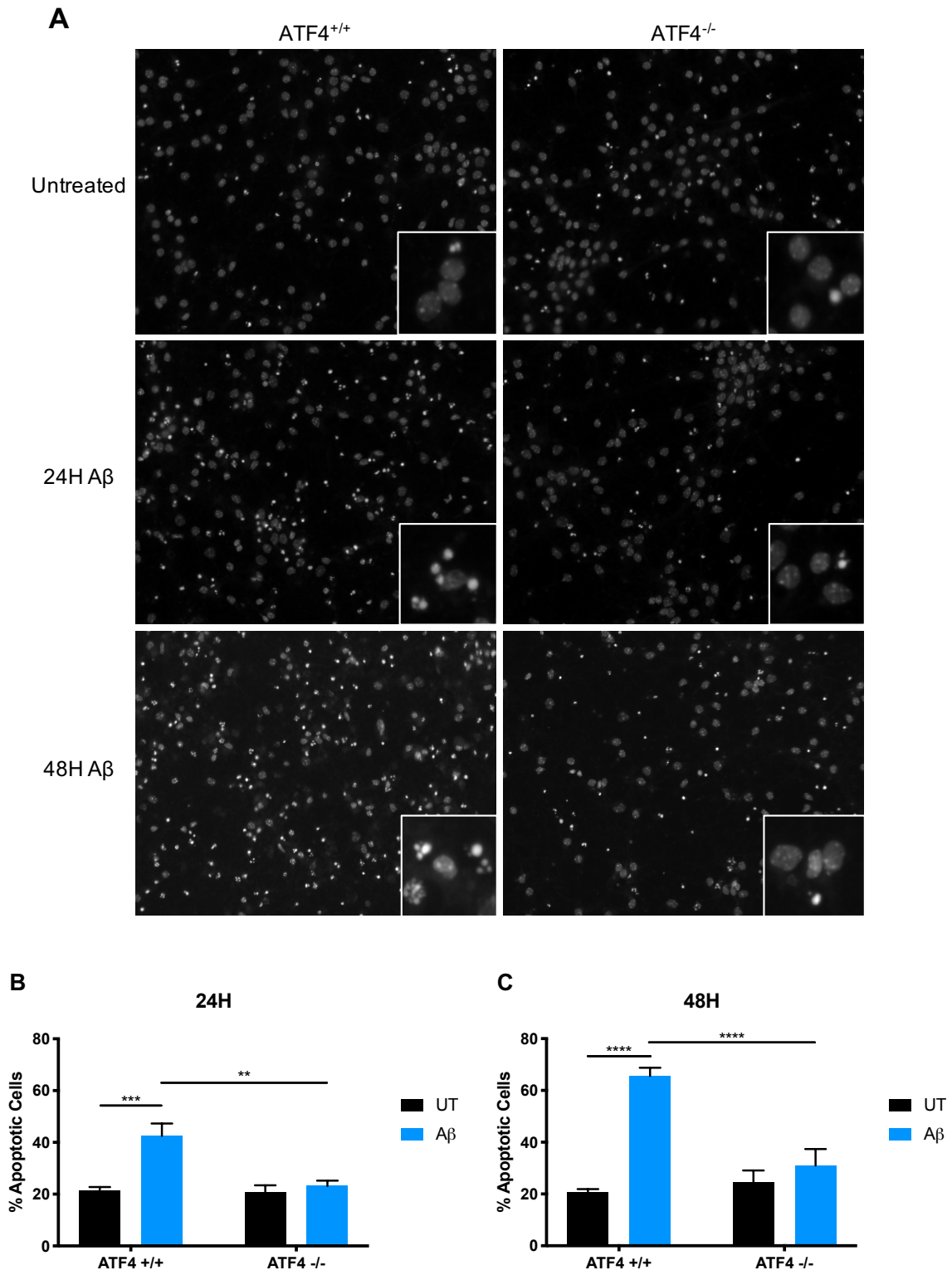


**Figure 3.6. ATF4 is necessary for amyloid- $\beta$ -induced apoptosis.** ATF4 wildtype and knockout cortical neurons were treated with and without 1  $\mu$ M amyloid- $\beta$  for 24 and 48 hours prior to being fixed and Hoechst stained. A) Representative images demonstrated increased apoptotic nuclear morphology in wildtype neurons treated with amyloid- $\beta$  at both time points. B) Following 24 hours of amyloid- $\beta$ , wildtype neurons displayed a significant increase in apoptotic nuclei compared to wildtype controls (\*\* $p < .001$ ;  $n = 7$ ). ATF4-deficient neurons ( $n = 6$ ) displayed significantly attenuated levels of apoptotic nuclei (\*\*  $p < .01$ ). C) ATF4 wildtype neurons treated with amyloid- $\beta$  for 48 hours showed more robust levels of apoptotic nuclei compared to wildtype controls (\*\*\*\*  $p < .0001$ ). ATF4-deficient neurons had attenuated levels of apoptosis (\*\*\*\*  $p < .0001$ ). Ordinary two-way ANOVAs and Tukey post-hoc tests were performed. Data are reported as mean percent apoptotic nuclei  $\pm$  SEM.

### 3.6 PUMA mediates neuronal apoptosis in an ATF4-dependent manner

In an effort to elucidate the apoptotic pathway induced by amyloid- $\beta$ , we focused on the BCL-2 protein family. More specifically, we focused on p53 upregulated mediator of apoptosis (PUMA), which is a BH3-only domain protein (Youle & Strasser, 2008). PUMA interacts with and inhibits the anti-apoptotic Bcl-2 family members, thus promoting apoptosis. Interaction of PUMA with the pro-apoptotic BCL-2 protein member BAX leads to outer mitochondrial membrane permeabilization and release of pro-apoptotic molecules. Subsequently, caspases are activated and induce apoptosis. Previously, our lab has demonstrated that PUMA can be activated through the induction of endoplasmic reticulum stress and oxidative stress (Galehdar et al., 2010; Steckley et al., 2007). Therefore, we hypothesized that amyloid- $\beta$  induces apoptosis in an ATF4- and PUMA-dependent manner.

#### 3.6.1 Amyloid- $\beta$ induces ATF4-dependent PUMA expression

We first examined the levels of PUMA transcript in ATF4<sup>+/+</sup> and ATF4<sup>-/-</sup> neurons following 12h of amyloid- $\beta$  treatment. ATF4 wildtype and knockout neurons showed no significant difference in PUMA expression under control conditions (Figure 3.7;  $p > .05$ ). Following 12h of A $\beta$  treatment, wildtype neurons displayed a large increase in PUMA expression compared to wildtype controls (\*\*\*) ( $p < .001$ ). PUMA levels were attenuated in ATF4 knockout neurons (\*\*  $p < .01$ ) and treated ATF4<sup>-/-</sup> neurons showed no difference in expression compared to ATF4<sup>-/-</sup> controls ( $p > .05$ ). We concluded that PUMA expression is induced in an ATF4-dependent manner following amyloid- $\beta$  treatment.

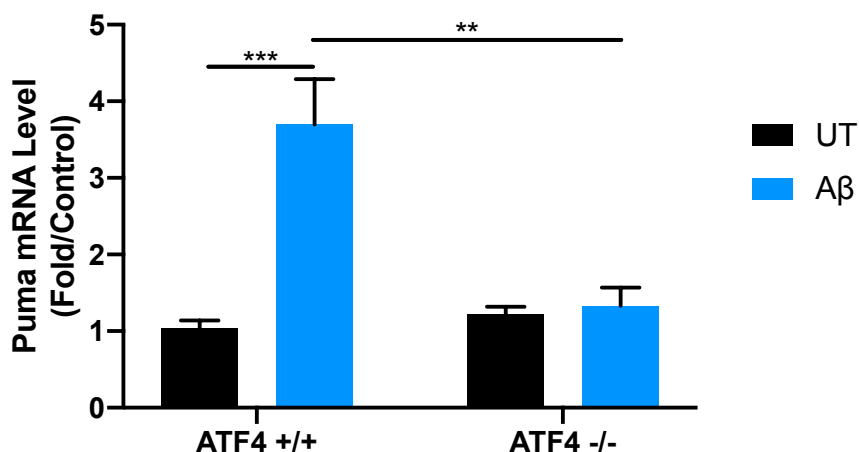


**Figure 3.7. PUMA expression is attenuated in ATF4-deficient neurons.** ATF4 wildtype and knockout neurons were treated with and without 1  $\mu$ M amyloid- $\beta$  for 12 hours prior to RNA isolation. qRT-PCR was performed probing for changes in PUMA expression. Amyloid- $\beta$  treatment increased PUMA expression in ATF4<sup>+/+</sup> neurons, which was attenuated in A $\beta$ -treated ATF4<sup>-/-</sup> neurons (\*\*  $p < .01$ ; \*\*\*  $p < .001$ ; \*\*\*\*). An ordinary two-way ANOVA and Tukey post-hoc tests were performed to determine statistical significance. Data are reported as mean  $\pm$  SEM of mRNA fold changes relative to untreated wildtype controls (ATF4<sup>+/+</sup>  $n = 9$ ; ATF4<sup>-/-</sup>  $n = 5$ ).

### 3.6.2 Caspase-mediated apoptosis is attenuated in PUMA-deficient neurons

Next, we investigated whether PUMA is required to mediate amyloid- $\beta$ -induced apoptosis. Increased expression and activity of PUMA induces the intrinsic apoptotic pathway and the release of soluble pro-apoptotic molecules from the mitochondrial intermembrane space (Willis et al., 2007). Cytochrome C is the best studied of these proteins, and its release from the mitochondria activates the formation of an apoptosome and the activation of caspases (Youle & Strasser, 2008). Cytochrome C serves as a marker of PUMA-dependent apoptosis. Using immunofluorescent staining, we investigated the retention of cytochrome C in PUMA<sup>+/+</sup> and PUMA<sup>-/-</sup> neurons treated with and without 1  $\mu$ M amyloid- $\beta$  for 48 hours (n = 3; Figure 3.8A). The percentage of cytochrome C-positive cells was significantly attenuated in PUMA<sup>+/+</sup> neurons (22.5%  $\pm$  2.6; \* p < .05; \*\* p < .01) compared to both PUMA<sup>+/+</sup> untreated neurons (64.0%  $\pm$  11.3) and PUMA<sup>-/-</sup> amyloid- $\beta$ -treated neurons (57.9%  $\pm$  4.5; Figure 3.8B). Additionally, the same PUMA<sup>-/-</sup> amyloid- $\beta$  treated neurons had a significantly greater percentage of apoptotic nuclei (68.6%  $\pm$  6.9; \*\* p < .01) compared to wildtype controls (24.9%  $\pm$  7.8) and PUMA-deficient amyloid- $\beta$  treated neurons (21.4%  $\pm$  5.2; Figure 3.8C), measured using Hoechst stain.

Following our cytochrome C results, we investigated caspase activity in PUMA<sup>+/+</sup>, PUMA<sup>+/-</sup> and PUMA<sup>-/-</sup> littermates. We investigated the activity of caspase-3, which lies downstream of PUMA and cytochrome C. Caspase-3 activation leads to irreversible commitment to apoptosis. A fluorescence-based caspase activity assay was performed using wildtype and heterozygous neurons (PUMA<sup>+/-</sup>; n = 7) compared to PUMA knockout neurons (n = 8). All neurons underwent treatment with and without amyloid- $\beta$  for 36 hours. No significant differences in caspase activity at baseline between genotypes were found (p > .05). Following amyloid- $\beta$  treatment, PUMA<sup>+/-</sup> neurons showed a robust increase in caspase activity compared to untreated controls (\*\* p < .01). Additionally, there was attenuation of caspase activity in A $\beta$ -treated PUMA<sup>-/-</sup> neurons (\* p < .05). Therefore, our cytochrome C and caspase activity assays determined that amyloid- $\beta$  induces neuronal death in a PUMA-dependent manner.



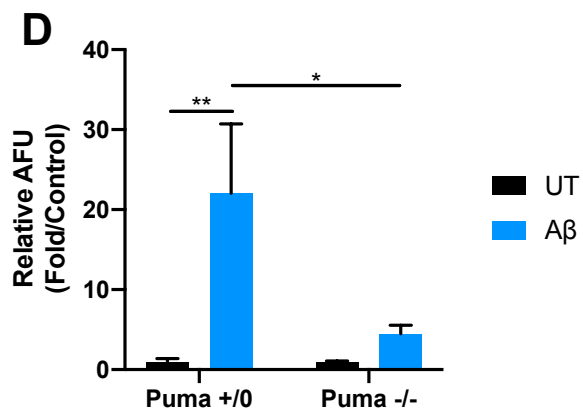
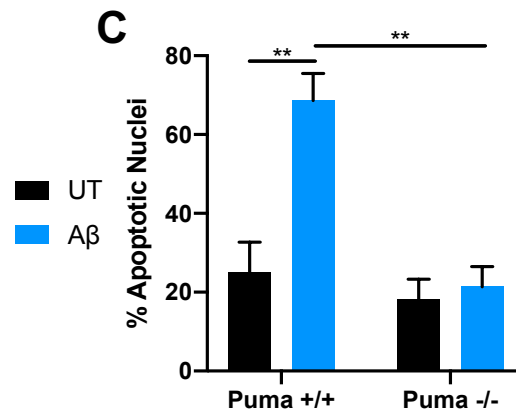
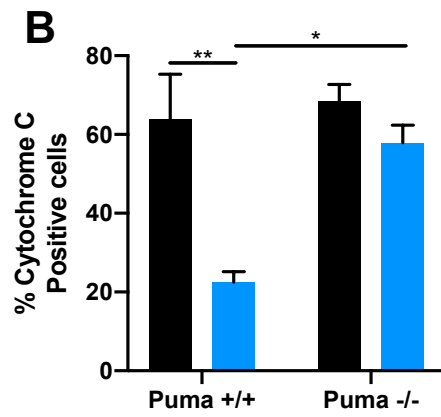
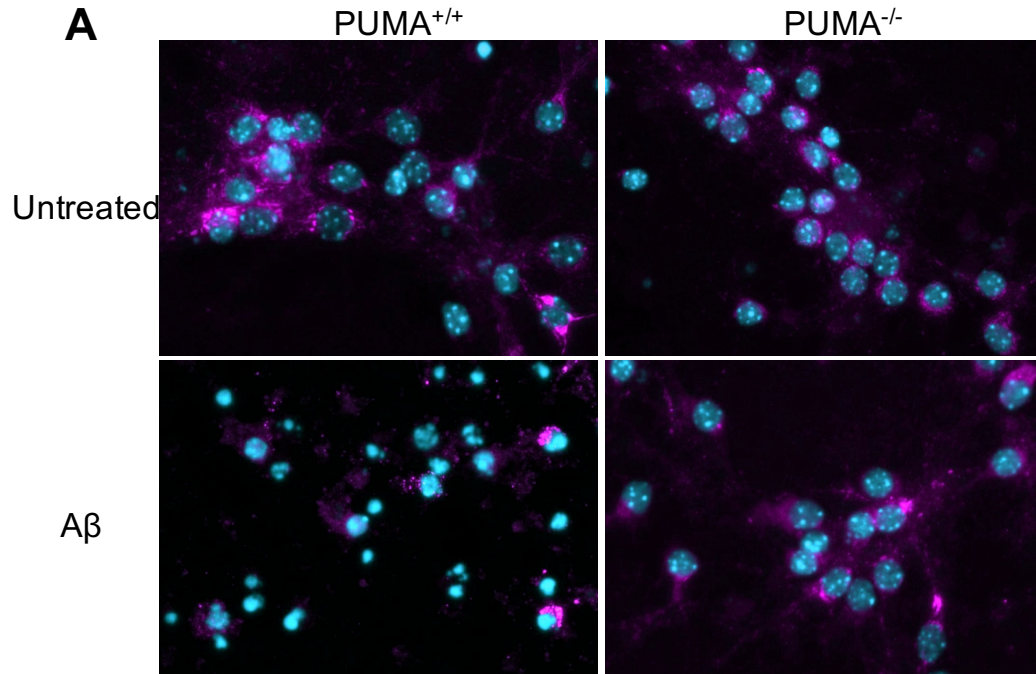


**Figure 3.8. Amyloid- $\beta$ -induced cell death occurs in a PUMA-dependent manner.** A) PUMA<sup>+/+</sup> and PUMA<sup>-/-</sup> neurons were treated with and without amyloid- $\beta$  for 48 hours prior to being fixed and immunostained for cytochrome C. Nuclei were visualized using Hoechst stain. B) PUMA<sup>+/+</sup> neurons had a significant reduction in cytochrome C-positive cells, which is indicative of mitochondrial-dependent apoptosis (\*\* p < .01). The percentage of cytochrome C positive cells in PUMA<sup>+/+</sup> neurons was attenuated compared to amyloid- $\beta$  treated PUMA-deficient neurons (\* p < .05). C) Apoptosis was significantly increased in A $\beta$ -treated wildtype neurons compared to wildtype controls and A $\beta$ -treated knockout neurons (\*\* p < .01). D) Caspase-3 activity was measured using a substrate that fluoresces when cleaved. Arbitrary fluorescence units (AFUs) were recorded and normalized to the mean AFU of PUMA<sup>+/-</sup> samples, thereby generating a fold change value relative to control. Caspase-3 activity was significantly increased following amyloid- $\beta$  treatment in PUMA<sup>+/-</sup> neurons (n = 7), compared to both untreated PUMA<sup>+/-</sup> neurons (\*\* p < .01) and amyloid- $\beta$ -treated PUMA-deficient neurons (\* p < .05; n = 8). Two-way ordinary ANOVA with Tukey post-hoc tests were performed for each data set to determine statistically significant differences between treatment groups and genotypes. Data reported are mean  $\pm$  SEM of the percent of cytochrome C-positive cells, the percent of apoptotic nuclei, and the relative AFU of caspase-3 activity.

## Chapter 4

### 4 Discussion

ATF4 is a member of the integrated stress response and its translation is paradoxically enhanced during periods of cellular stress when global protein translation is reduced (Harding et al., 2000). It is a bZIP transcription factor that modulates the expression of many stress-responsive genes involved in cellular processes such as autophagy, amino acid synthesis, and apoptosis (B'Chir et al., 2013; Harding et al., 2003). The wide range of transcription factors that ATF4 can heterodimerize with determine its transcriptional selectivity and the outcome of ISR signaling (Hai & Curran, 1991; Karpinski et al., 1992). Prolonged activation of the ISR and elevated levels of ATF4 have been shown to favour pro-death outcomes, specifically in neurons (Galehdar et al., 2010; Lange et al., 2008; Wortel et al., 2017). It has been well-documented in Alzheimer's disease and Alzheimer's disease paradigms that amyloid- $\beta$  induces high levels of neuronal stress (Deshpande et al., 2006). In the present study, we aimed to investigate the relationship between amyloid- $\beta$ , ATF4, and neuronal cell death. We provide evidence that (a) amyloid- $\beta$  induces ATF4 expression and neuronal death, that (b) amyloid- $\beta$ -induced death requires ATF4, and that (c) amyloid- $\beta$  induces death through a PUMA-dependent process in the presence of ATF4.

#### 4.1 Oligomeric Amyloid- $\beta$ induces ATF4 expression and apoptosis in neurons

Previously, it has been demonstrated that amyloid- $\beta$  induces high levels of neuronal stress *in vitro* and in *post mortem* samples from Alzheimer's disease patients (Baleriola et al., 2014; T. Ma et al., 2013). Markers of oxidative and endoplasmic reticulum stress have been measured in these samples. In the APP-PS1 mouse model of Alzheimer's disease, significant increases in the levels of phosphorylated eIF2 $\alpha$  were found in the hippocampus and prefrontal cortex (Ma et al., 2013). Elevated levels of ATF4 were found in the hippocampi of these animals. In human *post mortem* samples, high levels of phosphorylated eIF2 $\alpha$  were found in the hippocampus, mirroring the findings from the animal study (Ma et al., 2013). ATF4-positive cell bodies and axons were also found at a

higher frequency in the hippocampi of AD patients compared to age-matched controls (Baleriola et al., 2014). Chronic cellular stress results in the prolonged activation of the ISR and elevated levels of ATF4. Prolonged increases of ATF4 expression have been shown to favour pro-apoptotic cellular outcomes in neurons (Galehdar et al., 2010; Lange et al., 2008).

In the present study, primary cortical neurons extracted from embryonic mice were treated with oligomeric amyloid- $\beta$ . We found that amyloid- $\beta$  treatment induced a sustained increase in ATF4 protein expression, as well as a sustained increase in pro-apoptotic gene expression. We probed for changes in the mRNA expression of CHOP, Trib3, Gadd45 $\alpha$ , and 4eBP1. CHOP is a well-studied pro-apoptotic target gene of ATF4. In addition to CHOP being a target gene of ATF4 transcriptional regulation, CHOP is also able to heterodimerize with ATF4 and modulate the expression of many more genes. Research suggests that ectopic CHOP overexpression is sufficient to induce apoptotic death (Matsumoto, Minami, Takeda, Sakao, & Akira, 1996). Previous studies have found that Trib3, a pseudokinase, promotes apoptosis in neuronal cells (Aime et al., 2015; Lange et al., 2008; Ohoka et al., 2005). Trib3 expression is induced following both oxidative and endoplasmic reticulum stress, as well as in cellular models of Parkinson's disease. ATF4 and CHOP heterodimers have been shown to activate the Trib3 promoter and induce expression (Ohoka et al., 2005). Gadd45 $\alpha$  is a pro-death, stress-inducible protein. Research demonstrates that Gadd45 $\alpha$  promotes apoptosis by interacting with the BCL-2 protein family (Tong et al., 2005). Inducible expression of Gadd45 $\alpha$  in the absence of stress is sufficient to induce apoptosis. 4eBP1 is a translational repressor of the eIF4E complex involved in identifying the 5' cap of mRNA transcripts (Beugnet et al., 2003). Phosphorylation of 4eBP1 releases it from eIF4E and allows protein initiation to proceed. As mentioned previously, Alzheimer's disease can be characterized by aberrant cell death and synaptic dysfunction. *De novo* protein synthesis is essential to the maintenance of long-term potentiation, while cellular stress leads to a reduction in global protein translation through the ISR and phosphorylation of eIF2 $\alpha$ . The increase in 4eBP1 expression seen in response to amyloid- $\beta$  provides a second explanation for synaptic dysfunction in AD by inhibiting the translation of newly transcribed mRNA transcripts.

The results of the present study provide support that sustained upregulation of ATF4 favours pro-apoptotic cellular outcomes. We found a prolonged increase in ATF4 expression following treatment with amyloid- $\beta$ . Pro-apoptotic gene expression was robustly increased by treatment with A $\beta$ . Following 24 and 48 hours of amyloid- $\beta$  treatment, primary cortical neurons showed significantly elevated proportions of apoptotic nuclei compared to control-treated neurons. The number of apoptotic nuclei was even greater following 48 hours of amyloid- $\beta$  treatment compared to 24 hours of treatment. In addition, toxicity induced by amyloid- $\beta$  is specific to its amino acid sequence, as evaluated in the experiments using a scrambled version of the amyloid- $\beta$  peptide. The scrambled amyloid- $\beta$  peptide did not induce the expression of pro-apoptotic genes and did not induce apoptosis in primary cortical neurons. Therefore, treatment with amyloid- $\beta$  resulted in sustained ATF4 expression, increased transcription of stress-responsive pro-apoptotic genes, and apoptosis.

## 4.2 ATF4 is necessary for amyloid- $\beta$ -induced neuronal death

Following our experiments that determined oligomeric amyloid- $\beta$  induces ATF4 expression and leads to apoptosis, we wanted to further investigate the role that ATF4 plays in amyloid- $\beta$ -induced neuronal death. Our lab has previously shown that ATF4 promotes neuronal apoptosis in endoplasmic reticulum stress paradigms (Galehdar et al., 2010). Tunicamycin and thapsigargin, potent inducers of ER stress, induced apoptosis in an ATF4-dependent manner. ATF4-deficient neurons were more resistant toward ER-stress induced apoptosis (Galehdar et al., 2010). In the present study, ATF4-deficient primary cortical neurons were treated with and without amyloid- $\beta$ . The same pro-apoptotic genes were probed for changes in expression in wildtype and knockout neurons. Pro-apoptotic gene expression was attenuated in an ATF4-dependent manner. This provides evidence that CHOP, Trib3, Gadd45 $\alpha$ , and 4eBP1 are ATF4-responsive following treatment with amyloid- $\beta$ . ATF4-deficient neurons were also protected against amyloid- $\beta$ -induced apoptosis. Following both 24 and 48 hours of amyloid- $\beta$  treatment, ATF4 knockout neurons had attenuated apoptosis. Cell death experiments, together with

the results demonstrating attenuated pro-apoptotic gene expression in knockout neurons, led us to the conclusion that ATF4 is necessary for amyloid- $\beta$ -induced neuronal apoptosis. This has important implications for Alzheimer's disease, as aberrant cell death occurs as the disease progresses.

### 4.3 Amyloid- $\beta$ -induced death occurs through ATF4-mediated upregulation of PUMA

Previous work from our lab has demonstrated that BCL-2 family proteins play critical roles in the induction of oxidative stress and ER stress-induced apoptosis. The BCL-2 family is composed of pro-survival and pro-apoptotic proteins that interact to determine cell fate. PUMA is a BH3-only pro-apoptotic member of the BCL-2 family that has been extensively studied in our lab. PUMA was initially thought to be p53-dependent, however it is now known that it can be activated by both p53-dependent and -independent mechanisms (Galehdar et al., 2010). PUMA can be activated by endoplasmic reticulum and oxidative stress (Galehdar et al., 2010; Steckley et al., 2007). ER stress-induced PUMA expression occurs in an ATF4-dependent manner (Galehdar et al., 2010). In the present study we wanted to investigate the role that PUMA plays in amyloid- $\beta$ -induced neuronal death.

Following treatment with amyloid- $\beta$ , ATF4 wildtype neurons displayed a significant increase in PUMA mRNA expression. mRNA levels were attenuated in ATF4-deficient neurons. Next, primary cortical neurons were extracted from PUMA wildtype, heterozygous, and knockout neurons. In the mitochondrial apoptotic pathway, following activation, PUMA interacts indirectly or directly with other pro-apoptotic Bcl-2 members (Steckley et al., 2007; Willis et al., 2007). PUMA has been shown to activate the pro-apoptotic member BAX, which then translocates to the outer mitochondrial membrane. BAX causes permeabilization of the outer membrane and the release of soluble pro-apoptotic molecules into the cytoplasm, of which Cytochrome C is very well characterized (Kuwana et al., 2002). Cytochrome C release triggers formation of the apoptosome and the cleavage and subsequent activation of caspases (Li et al., 1997; Youle & Strasser, 2008). We investigated the retention of cytochrome C in PUMA

wildtype and knockout neurons following amyloid- $\beta$  treatment for 48 hours. PUMA<sup>+/+</sup> neurons displayed a significant reduction in cytochrome C positive cells post-treatment, as well as a significant increase in the percentage of apoptotic nuclei. PUMA-deficient neurons showed preservation of cytochrome C staining and an attenuation of apoptosis. A caspase-3 activity assay was performed using PUMA<sup>+0</sup> and PUMA<sup>-/-</sup> neurons following treatment with amyloid- $\beta$  for 36 hours. We found that the presence of even one allele of the PUMA gene was sufficient to induce robust caspase activity following amyloid- $\beta$  treatment. PUMA-deficient neurons displayed attenuated caspase-3 activity, which compliments the cytochrome C data found previously. PUMA-deficient neurons have retained cytochrome C within mitochondria, low activity of caspase-3, and attenuated apoptosis. Therefore, amyloid- $\beta$ -induced neuronal death occurs in a PUMA-dependent manner in the presence of ATF4.

#### 4.4 Implications of ATF4 in Alzheimer's disease

The present study highlights the important role that ATF4 has under an Alzheimer's disease-like paradigm. Excessive neuronal death and synaptic dysfunction are two cellular hallmarks that characterize Alzheimer's disease. ATF4 lies at the intersection between protein translation mechanisms and apoptosis, the latter being investigated in this study. Moving forward, it is important to continue elucidating the exact cascade that leads from extracellular amyloid- $\beta$  to ATF4 expression, and lastly to PUMA induction. In addition, future research should also focus on the role that ATF4 plays within the context of LTP and memory. Whole-embryo ATF4 knockout animals are not adequate for behavioural studies due to the developmental role of ATF4 in non-neuronal tissues. Brain-specific ATF4 knockout animals, or inducible brain-specific ATF4 knockout animals, should be used for studies of synaptic dysfunction and behaviour to limit the off-target effects of ATF4-deficiency.

## Chapter 5

### 5 Conclusion

Sustained upregulation of ATF4 has been shown to be pro-apoptotic in neurons, however the exact mechanism of ATF4-mediated death in response to amyloid- $\beta$  is not fully understood. Previous studies have suggested a relationship between Alzheimer's disease, oligomeric amyloid- $\beta$ , ATF4, and neuronal death. The findings of the present study support this paradigm, as well as provide a link between ATF4 and neuronal apoptosis (Figure 5.1). We found that oligomeric amyloid- $\beta$  induces neuronal apoptosis in an ATF4-dependent manner. Furthermore, we demonstrate that the expression of PUMA, a pro-apoptotic BCL-2 family member, is induced in the presence of ATF4. Amyloid- $\beta$  induces death through the intrinsic mitochondrial apoptotic pathway, since PUMA-deficient neurons are protected against amyloid- $\beta$ -induced death. Taken together, we conclude that amyloid- $\beta$ -induced neuronal death occurs in a PUMA-dependent manner in the presence of ATF4.



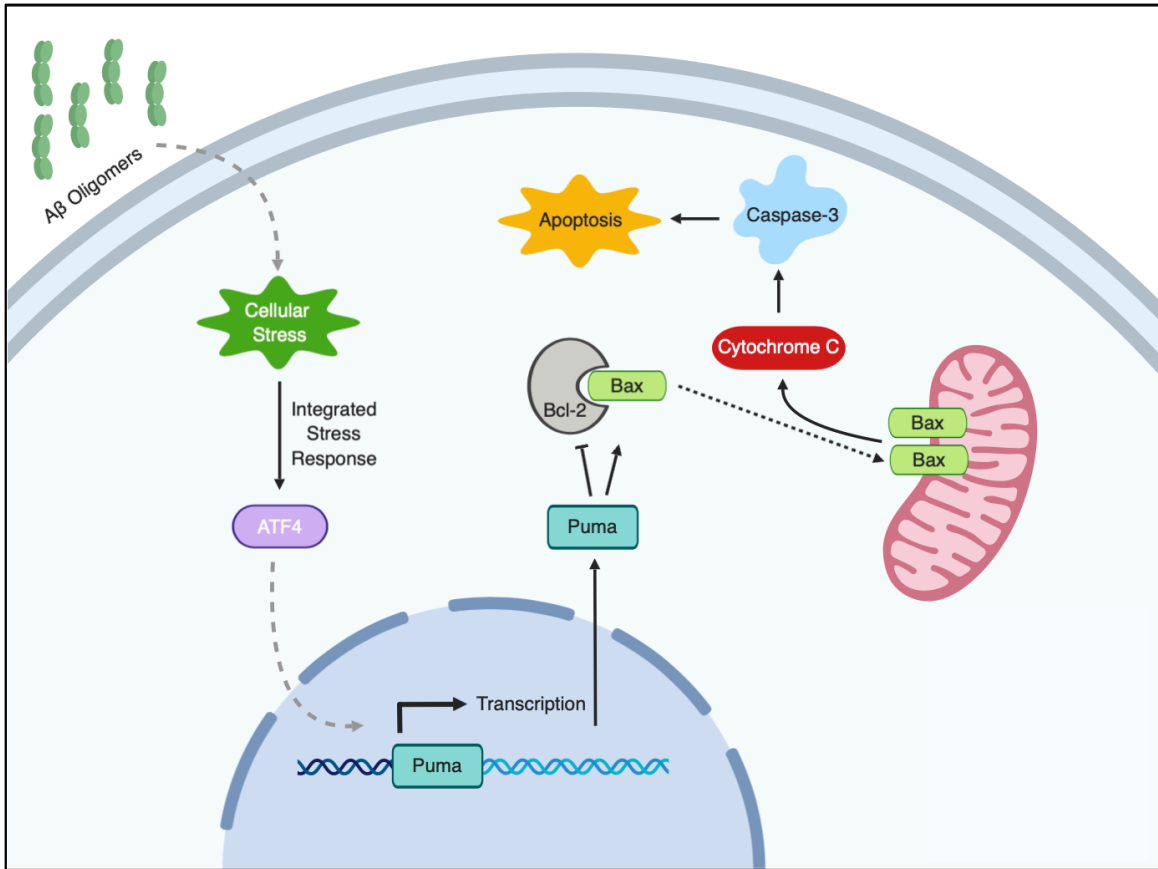


**Figure 5.1. Schematic of amyloid- $\beta$ -induced neuronal apoptosis.** We propose that amyloid- $\beta$  induces neuronal death through upregulation of ATF4 and subsequent induction of PUMA. PUMA indirectly or directly activates the pro-apoptotic protein BAX, which permeabilizes the outer mitochondrial membrane and releases cytochrome C into the cytoplasm. Cytochrome C subsequently activates caspase-3, culminating in apoptosis.

## References

- Aime, P., Sun, X., Zareen, N., Rao, A., Berman, Z., Volpicelli-Daley, L., ... Greene, L. A. (2015). Trib3 Is Elevated in Parkinson's Disease and Mediates Death in Parkinson's Disease Models. *Journal of Neuroscience*, *35*(30), 10731–10749. <https://doi.org/10.1523/JNEUROSCI.0614-15.2015>
- Ameri, K., & Harris, A. L. (2008). Activating transcription factor 4. *International Journal of Biochemistry and Cell Biology*, *40*(1), 14–21. <https://doi.org/10.1016/j.biocel.2007.01.020>
- Araki, W., Kitaguchi, N., Tokushima, Y., Ishii, K., Aratake, H., Shimohama, S., ... Kimura, J. (1991). Trophic effect of  $\beta$ -amyloid precursor protein on cerebral cortical neurons in culture. *Biochemical and Biophysical Research Communications*, *181*(1), 265–271. [https://doi.org/10.1016/S0006-291X\(05\)81412-3](https://doi.org/10.1016/S0006-291X(05)81412-3)
- B'Chir, W., Maurin, A. C., Carraro, V., Averous, J., Jousse, C., Muranishi, Y., ... Bruhat, A. (2013). The eIF2 $\alpha$ /ATF4 pathway is essential for stress-induced autophagy gene expression. *Nucleic Acids Research*, *41*(16), 7683–7699. <https://doi.org/10.1093/nar/gkt563>
- Baird, T. D., & Wek, R. C. (2012). *Eukaryotic Initiation Factor 2 Phosphorylation and Translational Control in Metabolism*. 307–321. <https://doi.org/10.3945/an.112.002113>.We
- Baleriola, J., Walker, C. A., Jean, Y. Y., Crary, J. F., Troy, C. M., Nagy, P. L., & Hengst, U. (2014). Axonally synthesized ATF4 transmits a neurodegenerative signal across brain regions. *Cell*, *158*(5), 1159–1172. <https://doi.org/10.1016/j.cell.2014.07.001>
- Bentahir, M., Nyabi, O., Verhamme, J., Tolia, A., Horr , K., Wiltfang, J., ... De Strooper, B. (2006). Presenilin clinical mutations can affect  $\gamma$ -secretase activity by different mechanisms. *Journal of Neurochemistry*, *96*(3), 732–742. <https://doi.org/10.1111/j.1471-4159.2005.03578.x>

- Beugnet, A., Wang, X., & Proud, C. G. (2003). Target of Rapamycin (TOR)-signaling and RAIP Motifs Play Distinct Roles in the Mammalian TOR-dependent Phosphorylation of Initiation Factor 4E-binding Protein. *Journal of Biological Chemistry*, 278(42), 40717–40722. <https://doi.org/10.1074/jbc.M308573200>
- Bi, M., Naczki, C., Koritzinsky, M., Fels, D., Blais, J., Hu, N., ... Koumenis, C. (2005). ER stress-regulated translation increases tolerance to extreme hypoxia and promotes tumor growth. *The EMBO Journal*, 24(19), 3470–3481. <https://doi.org/10.1038/sj.emboj.7600777>
- Bitan, G., Kirkitadze, M. D., Lomakin, A., Vollers, S. S., Benedek, G. B., & Teplow, D. B. (2002). *Amyloid beta-protein (AB) assembly - AB40 and AB42 oligomerize through distinct.pdf*. Retrieved from [www.pnas.org](http://www.pnas.org).
- Bliss, T. V., & Collingridge, G. L. (1993). A synaptic model of memory: long-term potentiation in the hippocampus. *Nature*, 361(6407), 31–39. <https://doi.org/10.1038/361031a0>
- Bliss, T. V., & Lomo, T. (1973). Long-lasting potentiation of synaptic transmission in the dentate area of the anaesthetized rabbit following stimulation of the perforant path. *The Journal of Physiology*, 232(2), 331–356. <https://doi.org/10.1113/jphysiol.1973.sp010273>
- Braak, H., & Braak, E. (1991). Neuropathological staging of Alzheimer-related changes. *Acta Neuropathologica*, 239–259.
- Caccamo, A., Oddo, S., Sugarman, M. C., Akbari, Y., & LaFerla, F. M. (2005). Age- and region-dependent alterations in A $\beta$ -degrading enzymes: Implications for A $\beta$ -induced disorders. *Neurobiology of Aging*, 26(5), 645–654. <https://doi.org/10.1016/j.neurobiolaging.2004.06.013>
- Carrara, M., Prischi, F., Nowak, P. R., Kopp, M. C., & Ali, M. M. (2015). Noncanonical binding of BiP ATPase domain to Ire1 and Perk is dissociated by unfolded protein CH1 to initiate ER stress signaling. *ELife*, 2015(4). <https://doi.org/10.7554/eLife.03522>

- Chambers, L. W., Bancej, C., & McDowell, I. (2016). The Alzheimer Society of Canada. *Prevalence and Monetary Costs of Dementia in Canada: Population Health Expert Panel*.
- Chang, R. C. C., Wong, A. K. Y., Ng, H. K., & Hugon, J. (2002). Phosphorylation of eukaryotic initiation factor-2a (eIF2a) is associated with neuronal degeneration in Alzheimer's disease. *NeuroReport*, *13*(18), 2429–2432.  
<https://doi.org/10.1097/00001756-200212200-00011>
- Chen, A., Muzzio, I. A., Malleret, G., Bartsch, D., Verbitsky, M., Pavlidis, P., ... Kandel, E. R. (2003). Inducible enhancement of memory storage and synaptic plasticity in transgenic mice expressing an inhibitor of ATF4 (CREB-2) and C/EBP proteins. *Neuron*, *39*(4), 655–669. [https://doi.org/10.1016/S0896-6273\(03\)00501-4](https://doi.org/10.1016/S0896-6273(03)00501-4)
- Chen, G. F., Xu, T. H., Yan, Y., Zhou, Y. R., Jiang, Y., Melcher, K., & Xu, H. E. (2017). Amyloid beta: Structure, biology and structure-based therapeutic development. *Acta Pharmacologica Sinica*, *38*(9), 1205–1235. <https://doi.org/10.1038/aps.2017.28>
- Chen, J. J., Throop, M. S., Gehrke, L., Kuo, I., Pal, J. K., Brodsky, M., & London, I. M. (1991). Cloning of the cDNA of the heme-regulated eukaryotic initiation factor 2 alpha (eIF-2 alpha) kinase of rabbit reticulocytes: homology to yeast GCN2 protein kinase and human double-stranded-RNA-dependent eIF-2 alpha kinase. *Proceedings of the National Academy of Sciences*, *88*(17), 7729–7733.  
<https://doi.org/10.1073/pnas.88.17.7729>
- Chen, T., Ozel, D., Qiao, Y., Harbinski, F., Chen, L., Denoyelle, S., ... Aktas, B. H. (2013). Chemical genetics identify eIF2 $\alpha$  kinase heme-regulated inhibitor as an anticancer target. *Nature Chemical Biology*, *7*(9), 610–616.  
<https://doi.org/10.1038/nchembio.613>
- Choi, H. J., Kang, K. S., Fukui, M., & Zhu, B. T. (2011). Critical role of the JNK-p53-GADD45 $\alpha$  apoptotic cascade in mediating oxidative cytotoxicity in hippocampal neurons. *British Journal of Pharmacology*, *162*(1), 175–192.  
<https://doi.org/10.1111/j.1476-5381.2010.01041.x>

- Costa-Mattioli, M., Gobert, D., Harding, H. P., Herdy, B., Mounia, A., Bruno, M., ... Sonenberg, N. (2005). Translational control of hippocampal synaptic plasticity and memory by the eIF2 $\alpha$  kinase, GCN2. *Nature*.
- Costa-Mattioli, M., Gobert, D., Stern, E., Gamache, K., Colina, R., Cuello, A. C., ... Sonenberg, N. (2007). eIF2 $\alpha$  phosphorylation bidirectionally regulates the switch from short to long-term synaptic plasticity and memory. *Cell*, 32(7), 195–206. <https://doi.org/10.1371/journal.pone.0178059>
- Cregan, S. P., Arbour, N. A., MacLaurin, J. G., Callaghan, S. M., Fortin, A., Cheung, E. C. C., ... Slack, R. S. (2004). p53 Activation Domain 1 Is Essential for PUMA Upregulation and p53-Mediated Neuronal Cell Death. *Journal of Neuroscience*, 24(44), 10003–10012. <https://doi.org/10.1523/jneurosci.2114-04.2004>
- Das, S., Maiti, T., Das, K., & Maitra, U. (1997). Specific Interaction of Eukaryotic Translation Initiation Factor (eIF5) with the b-Subunit of eIF2. *The Journal of Biological Chemistry*, 272(50), 31712–31718. Retrieved from <http://www.jbc.org/>
- De Pietri Tonelli, D., Mihailovich, M., Di Cesare, A., Codazzi, F., Grohovaz, F., & Zacchetti, D. (2004). Translational regulation of BACE-1 expression in neuronal and non-neuronal cells. *Nucleic Acids Research*, 32(5), 1808–1817. <https://doi.org/10.1093/nar/gkh348>
- De Strooper, B. (2003, April). Aph-1, Pen-2, and Nicastrin with Presenilin generate an active  $\gamma$ -Secretase complex. *Neuron*, Vol. 38, pp. 9–12. [https://doi.org/10.1016/S0896-6273\(03\)00205-8](https://doi.org/10.1016/S0896-6273(03)00205-8)
- Deshpande, A., Mina, E., Glabe, C., & Busciglio, J. (2006). Different Conformations of Amyloid beta Induce Neurotoxicity by Distinct Mechanisms in Human Cortical Neurons. *Journal of Neuroscience*, 26(22), 6011–6018. <https://doi.org/10.1523/jneurosci.1189-06.2006>

- Deval, C., Chaveroux, C., Maurin, A. C., Cherasse, Y., Parry, L., Carraro, V., ... Fafournoux, P. (2009). Amino acid limitation regulates the expression of genes involved in several specific biological processes through GCN2-dependent and GCN2-independent pathways. *FEBS Journal*, *276*(3), 707–718. <https://doi.org/10.1111/j.1742-4658.2008.06818.x>
- Devi, L., & Ohno, M. (2014). *PERK mediates eIF2 $\alpha$  phosphorylation responsible for BACE1 elevation, CREB dysfunction and neurodegeneration in a mouse model of Alzheimer's disease*. *71*(2), 2272–2281. <https://doi.org/10.1038/mp.2011.182>.doi
- Dey, S., Baird, T. D., Zhou, D., Palam, L. R., Spandau, D. F., & Wek, R. C. (2010). Both transcriptional regulation and translational control of ATF4 are central to the integrated stress response. *Journal of Biological Chemistry*, *285*(43), 33165–33174. <https://doi.org/10.1074/jbc.M110.167213>
- Donnelly, N., Gorman, A. M., Gupta, S., & Samali, A. (2013). The eIF2 $\alpha$  kinases: Their structures and functions. *Cellular and Molecular Life Sciences*, *70*(19), 3493–3511. <https://doi.org/10.1007/s00018-012-1252-6>
- Duering, M., Grimm, M. O. W., Grimm, H. S., Schröder, J., & Hartmann, T. (2005). Mean age of onset in familial Alzheimer's disease is determined by amyloid beta 42. *Neurobiology of Aging*, *26*(6), 785–788. <https://doi.org/10.1016/j.neurobiolaging.2004.08.002>
- Farrow, T. F. D., Thiyaresh, S. N., Wilkinson, I. D., Parks, R. W., Ingram, L., & Woodruff, P. W. R. (2007). Fronto-temporal-lobe atrophy in early-stage Alzheimer's disease identified using an improved detection methodology. *Psychiatry Research - Neuroimaging*, *155*(1), 11–19. <https://doi.org/10.1016/j.psychresns.2006.12.013>
- Fawcett, T. W., Martindale, J. L., Guyton, K. Z., Hai, T., & Holbrook, N. J. (1999). Complexes containing activating transcription factor (ATF)/cAMP-responsive-element-binding protein (CREB) interact with the CCAAT/enhancer-binding protein (C/EBP)-ATF composite site to regulate Gadd153 expression during the stress response. *Biochem J*, *339*, 135–141. [https://doi.org/10.1016/s1095-6433\(99\)90422-1](https://doi.org/10.1016/s1095-6433(99)90422-1)

- Fernandez, J., Yaman, I., Sarnow, P., Snider, M. D., & Hatzoglou, M. (2002). Regulation of internal ribosomal entry site-mediated translation by phosphorylation of the translation initiation factor eIF2 $\alpha$ . *Journal of Biological Chemistry*, 277(21), 19198–19205. <https://doi.org/10.1074/jbc.M201052200>
- Fischer, C., Johnson, J., Stillwell, B., Conner, J., Cerovac, Z., Wilson-Rawls, J., & Rawls, A. (2004). Activating Transcription Factor 4 Is Required for the Differentiation of the Lamina Propria Layer of the Vas Deferens1. *Biology of Reproduction*, 70(2), 371–378. <https://doi.org/10.1095/biolreprod.103.021600>
- Fukumoto, H., Cheung, B. S., Hyman, B. T., & Irizarry, M. C. (2002).  $\beta$ -secretase protein and activity are increased in the neocortex in Alzheimer disease. *Archives of Neurology*, 59(9), 1381–1389. <https://doi.org/10.1001/archneur.59.9.1381>
- Galehdar, Z., Swan, P., Fuerth, B., Callaghan, S. M., Park, D. S., & Cregan, S. P. (2010). Neuronal Apoptosis Induced by Endoplasmic Reticulum Stress Is Regulated by ATF4-CHOP-Mediated Induction of the Bcl-2 Homology 3-Only Member PUMA. *Journal of Neuroscience*, 30(50), 16938–16948. <https://doi.org/10.1523/JNEUROSCI.1598-10.2010>
- Ghosh, A. P., Klocke, B. J., Ballestas, M. E., & Roth, K. A. (2012). CHOP potentially cooperates with FOXO3a in neuronal cells to regulate PUMA and BIM expression in response to ER stress. *PloS One*, 7(6), e39586. <https://doi.org/10.1371/journal.pone.0039586>
- Gingras, A.-C., Raught, B., & Sonenberg, N. (2002). eIF4 Initiation Factors: Effectors of mRNA Recruitment to Ribosomes and Regulators of Translation. *Annual Review of Biochemistry*, 68(1), 913–963. <https://doi.org/10.1146/annurev.biochem.68.1.913>
- Gomez, E., Mohammad, S. S., & Pavitt, G. D. (2002). Characterization of the minimal catalytic domain within eIF2B: The guanine-nucleotide exchange factor for translation initiation. *EMBO Journal*, 21(19), 5292–5301. <https://doi.org/10.1093/emboj/cdf515>

- Gouras, G. K., Olsson, T. T., & Hansson, O. (2015). beta-Amyloid peptides and amyloid plaques in Alzheimer's disease. *Neurotherapeutics : The Journal of the American Society for Experimental NeuroTherapeutics*, 12(1), 3–11.  
<https://doi.org/10.1007/s13311-014-0313-y>
- Guix, F. X., Sartório, C. L., & ILL-Raga, G. (2019). BACE1 Translation: At the Crossroads Between Alzheimer's Disease Neurodegeneration and Memory Consolidation. *Journal of Alzheimer's Disease Reports*, 3(1), 113–148.  
<https://doi.org/10.3233/adr-180089>
- Haass, Christian, Lemere, C. A., Capell, A., Citron, M., Seubert, P., Schenk, D., ... Selkoe, D. J. (1995). The Swedish mutation causes early-onset Alzheimer's disease by  $\beta$ -secretase cleavage within the secretory pathway. *Nature Medicine*, 1(12), 1291–1296. <https://doi.org/10.1038/nm1295-1291>
- Haass, Christian, & Selkoe, D. J. (1993, December). Cellular processing of  $\beta$ -amyloid precursor protein and the genesis of amyloid  $\beta$ -peptide. *Cell*, Vol. 75, pp. 1039–1042. [https://doi.org/10.1016/0092-8674\(93\)90312-E](https://doi.org/10.1016/0092-8674(93)90312-E)
- Haass, Christian, & Selkoe, D. J. (2007). Soluble protein oligomers in neurodegeneration: Lessons from the Alzheimer's amyloid  $\beta$ -peptide. *Nature Reviews Molecular Cell Biology*, 8(2), 101–112. <https://doi.org/10.1038/nrm2101>
- Haass, Christina, Schlossmacher, M. G., Hung, A. Y., Vigo-Pelfrey, C., Mellon, A., Ostaszewski, B. L., ... Selkoe, D. J. (1992). Amyloid  $\beta$ -peptide is produced by cultured cells during normal metabolism. *Nature*, 359(6393), 322–325.  
<https://doi.org/10.1038/359322a0>
- Hai, T., & Curran, T. (1991). Cross-family dimerization of transcription factors Fos/Jun and ATF/CREB alters DNA binding specificity. *Proceedings of the National Academy of Sciences*, 88, 3720–3724.
- Hai, T., Liu, F., Coukos, W. J., & Green, M. R. (1989). Transcription factor ATF cDNA clones: An extensive family of leucine zipper proteins able to selectively form DNA-binding heterodimers. *Genes and Development*, 3(12 B), 2083–2090.  
<https://doi.org/10.1101/gad.3.12b.2083>



- Han, J., Back, S. H., Hur, J., Lin, Y. H., Gildersleeve, R., Shan, J., ... Kaufman, R. J. (2013). ER-stress-induced transcriptional regulation increases protein synthesis leading to cell death. *Nature Cell Biology*, *15*(5), 481–490.  
<https://doi.org/10.1038/ncb2738>
- Harding, H. P., Novoa, I., Zhang, Y., Zeng, H., Wek, R., Schapira, M., & Ron, D. (2000). Stress-Induced Gene Expression in Mammalian Cells. *Molecular Cell*, *6*, 1099–1108. [https://doi.org/S1097-2765\(00\)00108-8](https://doi.org/S1097-2765(00)00108-8) [pii]
- Harding, H. P., Zhang, Y., Zeng, H., Novoa, I., Lu, P. D., Calfon, M., ... Carolina, N. (2003). An Integrated Stress Response Regulates Amino Acid Metabolism and Resistance to Oxidative Stress. *Molecular Cell*, *11*, 619–633. Retrieved from <http://www.molecule.org/>
- Harris, J. A., Devidze, N., Verret, L., Ho, K., Halabisky, B., Thwin, M. T., ... Mucke, L. (2010). Transsynaptic Progression of Amyloid- $\beta$ -Induced Neuronal Dysfunction within the Entorhinal-Hippocampal Network. *Neuron*, *68*(3), 428–441.  
<https://doi.org/10.1016/j.neuron.2010.10.020>
- Hay, N., & Sonenberg, N. (2004, August 15). Upstream and downstream of mTOR. *Genes and Development*, Vol. 18, pp. 1926–1945.  
<https://doi.org/10.1101/gad.1212704>
- Hettmann, T., Barton, K., & Leiden, J. M. (2000). Microphthalmia due to p53-mediated apoptosis of anterior lens epithelial cells in mice lacking the CREB-2 transcription factor. *Developmental Biology*, *222*(1), 110–123.  
<https://doi.org/10.1006/dbio.2000.9699>
- Hinnebusch, A. G., & Lorsch, J. R. (2012). The mechanism of eukaryotic translation initiation: New insights and challenges. *Cold Spring Harbor Perspectives in Biology*, *4*(10). <https://doi.org/10.1101/cshperspect.a011544>
- Iwata, N., Tsubuki, S., Takaki, Y., Watanabe, K., Sekiguchi, M., Hosoki, E., ... Saido, T. (2000). Identification of the major amyloid-beta-1-42-degrading catabolic pathway in brain parenchyma: suppression leads to biochemical and pathological deposition. *Nature Medicine*, *6*(2), 143–149.

- Iwatsubo, T. (2004, June). The  $\gamma$ -secretase complex: Machinery for intramembrane proteolysis. *Current Opinion in Neurobiology*, Vol. 14, pp. 379–383.  
<https://doi.org/10.1016/j.conb.2004.05.010>
- Joshi, A. U., Kornfeld, O. S., & Mochly-Rosen, D. (2016). The entangled ER-mitochondrial axis as a potential therapeutic strategy in neurodegeneration: A tangled duo unchained. *Cell Calcium*, 60(3), 218–234.  
<https://doi.org/10.1016/j.ceca.2016.04.010>
- Kang, J., Lemaire, H.-G., Unterbeck, A., Salbaum, J. M., Masters, C. L., Grzeschik, K.-H., ... Müller-Hill, B. (1987). The precursor of Alzheimer's disease amyloid A4 protein resembles a cell-surface receptor. *Nature*, 325(6106), 733–736.  
<https://doi.org/10.1038/325733a0>
- Karpinski, B. A., Morle, G. D., Huggenvik, J., Uhler, M. D., & Leiden, J. M. (1992). Molecular cloning of human CREB-2: an ATF/CREB transcription factor that can negatively regulate transcription from the cAMP response element. *Proceedings of the National Academy of Sciences*, 89(11), 4820–4824.  
<https://doi.org/10.1073/pnas.89.11.4820>
- Kimball, S. R. (1997). Eukaryotic initiation factor eIF2. *International Journal of Biochemistry and Cell Biology*, 29(10), 1127–1131. [https://doi.org/10.1016/S1357-2725\(97\)00039-3](https://doi.org/10.1016/S1357-2725(97)00039-3)
- Kimberly, W. T., LaVoie, M. J., Ostaszewski, B. L., Ye, W., Wolfe, M. S., & Selkoe, D. J. (2003).  $\gamma$ -Secretase is a membrane protein complex comprised of presenilin, nicastrin, aph-1, and pen-2. *Proceedings of the National Academy of Sciences*, 100(11), 6382–6387. <https://doi.org/10.1073/pnas.1037392100>
- Köditz, J., Nesper, J., Wottawa, M., Stiehl, D. P., Camenisch, G., Franke, C., ... Katschinski, D. M. (2007). Oxygen-dependent ATF-4 stability is mediated by the PHD3 oxygen sensor. *Blood*, 110(10), 3610–3617. <https://doi.org/10.1182/blood-2007-06-094441>

- Krishnamoorthy, T., Pavitt, G. D., Zhang, F., Dever, T. E., & Hinnebusch, A. G. (2001). Tight Binding of the Phosphorylated Subunit of Initiation Factor 2 (eIF2) to the Regulatory Subunits of Guanine Nucleotide Exchange Factor eIF2B Is Required for Inhibition of Translation Initiation. *Molecular and Cellular Biology*, 21(15), 5018–5030. <https://doi.org/10.1128/mcb.21.15.5018-5030.2001>
- Kuwana, T., Mackey, M. R., Perkins, G., Ellisman, M. H., Latterich, M., Schneider, R., ... Newmeyer, D. D. (2002). Bid, Bax, and lipids cooperate to form supramolecular openings in the outer mitochondrial membrane. *Cell*, 111(3), 331–342. [https://doi.org/10.1016/S0092-8674\(02\)01036-X](https://doi.org/10.1016/S0092-8674(02)01036-X)
- Lammich, S., Schöbel, S., Zimmer, A. K., Lichtenthaler, S. F., & Haass, C. (2004). Expression of the Alzheimer protease BACE1 is suppressed via its 5'-untranslated region. *EMBO Reports*, 5(6), 620–625. <https://doi.org/10.1038/sj.embor.7400166>
- Lange, P. S., Chavez, J. C., Pinto, J. T., Coppola, G., Sun, C.-W., Townes, T. M., ... Ratan, R. R. (2008). ATF4 is an oxidative stress-inducible, prodeath transcription factor in neurons in vitro and in vivo. *The Journal of Experimental Medicine*, 205(5), 1227–1242. <https://doi.org/10.1084/jem.20071460>
- Lassot, I., Estrabaud, E., Emiliani, S., Benkirane, M., Benarous, R., & Margottin-Goguet, F. (2005). p300 modulates ATF4 stability and transcriptional activity independently of its acetyltransferase domain. *Journal of Biological Chemistry*, 280(50), 41537–41545. <https://doi.org/10.1074/jbc.M505294200>
- Lassot, I., Segéral, E., Berlioz-Torrent, C., Durand, H., Groussin, L., Hai, T., ... Margottin-Goguet, F. (2001). ATF4 Degradation Relies on a Phosphorylation-Dependent Interaction with the SCF TrCP Ubiquitin Ligase. *Molecular and Cellular Biology*, 21(6), 2192–2202. <https://doi.org/10.1128/mcb.21.6.2192-2202.2001>
- Lee, A. S. (2001, August). The glucose-regulated proteins: Stress induction and clinical applications. *Trends in Biochemical Sciences*, Vol. 26, pp. 504–510. [https://doi.org/10.1016/S0968-0004\(01\)01908-9](https://doi.org/10.1016/S0968-0004(01)01908-9)

- Lesne, S., Ali, C., Gabriel, C., Croci, N., MacKenzie, E. T., Glabe, C. G., ... Buisson, A. (2005). NMDA Receptor Activation Inhibits  $\beta$ -Secretase and Promotes Neuronal Amyloid- Production. *Journal of Neuroscience*, *25*(41), 9367–9377.  
<https://doi.org/10.1523/jneurosci.0849-05.2005>
- Li, P., Nijhawan, D., Budihardjo, I., Srinivasula, S. M., Ahmad, M., Alnemri, E. S., & Wang, X. (1997). Cytochrome c and dATP-dependent formation of Apaf-1/caspase-9 complex initiates an apoptotic protease cascade. *Cell*, *91*(4), 479–489.  
[https://doi.org/10.1016/S0092-8674\(00\)80434-1](https://doi.org/10.1016/S0092-8674(00)80434-1)
- Lu, P. D., Harding, H. P., & Ron, D. (2004). Translation reinitiation at alternative open reading frames regulates gene expression in an integrated stress response. *Journal of Cell Biology*, *167*(1), 27–33. <https://doi.org/10.1083/jcb.200408003>
- Luo, S., Baumeister, P., Yang, S., Abcouwer, S. F., & Lee, A. S. (2003). Induction of Grp78/BiP by Translational Block. *Journal of Biological Chemistry*, *278*(39), 37375–37385. <https://doi.org/10.1074/jbc.m303619200>
- Lytton, J., Westlin, M., & Hanley, R. (1991). *Thapsigargin Inhibits the SERCA family of calcium pumps*. *266*(26), 17067–17071. Retrieved from <http://www.jbc.org.proxy1.lib.uwo.ca/content/266/26/17067.full.pdf>
- Ma, T., Trinh, M. A., Wexler, A. J., Bourbon, C., Gatti, E., Pierre, P., ... Klann, E. (2013). Suppression of eIF2 $\alpha$  kinases alleviates Alzheimer's disease-related plasticity and memory deficits. *Nature Neuroscience*, *16*(9), 1299–1305.  
<https://doi.org/10.1038/nn.3486>
- Ma, X. M., & Blenis, J. (2009). Molecular mechanisms of mTOR-mediated translational control. *Nature Reviews Molecular Cell Biology*, Vol. 10, pp. 307–318.  
<https://doi.org/10.1038/nrm2672>
- Ma, Y., & Hendershot, L. M. (2003). Delineation of a negative feedback regulatory loop that controls protein translation during endoplasmic reticulum stress. *Journal of Biological Chemistry*, *278*(37), 34864–34873.  
<https://doi.org/10.1074/jbc.M301107200>

- Masliah, E., Mallory, M., Hansen, L., Richard, D. T., Alford, M., & Terry, R. (1994). Synaptic and neuritic alterations during the progression of Alzheimer's disease. *Neuroscience Letters*, *174*(1), 67–72. [https://doi.org/10.1016/0304-3940\(94\)90121-X](https://doi.org/10.1016/0304-3940(94)90121-X)
- Masuoka, H. C., & Townes, T. M. (2002). Targeted disruption of the activating transcription factor 4 gene results in severe fetal anemia in mice. *Blood*, *99*(3), 736–746.
- Matsumoto, M., Minami, M., Takeda, K., Sakao, Y., & Akira, S. (1996). Ectopic expression of CHOP (GADD153) induces apoptosis in M1 myeloblastic leukemia cells. *FEBS Letters*, *395*(2–3), 143–147. [https://doi.org/10.1016/0014-5793\(96\)01016-2](https://doi.org/10.1016/0014-5793(96)01016-2)
- Miners, J. S., Van Helmond, Z., Chalmers, K., Wilcock, G., Love, S., & Kehoe, P. G. (2006). Decreased expression and activity of neprilysin in Alzheimer disease are associated with cerebral amyloid angiopathy. *Journal of Neuropathology and Experimental Neurology*, *65*(10), 1012–1021. Retrieved from isi:000241692600009
- Mitsuda, T., Hayakawa, Y., Itoh, M., Ohta, K., & Nakagawa, T. (2007). ATF4 regulates  $\gamma$ -secretase activity during amino acid imbalance. *Biochemical and Biophysical Research Communications*, *352*(3), 722–727. <https://doi.org/10.1016/j.bbrc.2006.11.075>
- Moore, C. E., Omikorede, O., Gomez, E., Willars, G. B., & Herbert, T. P. (2011). PERK Activation at Low Glucose Concentration Is Mediated by SERCA Pump Inhibition and Confers Preemptive Cytoprotection to Pancreatic  $\beta$ -Cells. *Molecular Endocrinology*, *25*(2), 315–326. <https://doi.org/10.1210/me.2010-0309>
- Murphy, M. P., & Levine, H. I. (2010). Alzheimer's Disease and the Beta-Amyloid Peptide. *Journal of Alzheimer's Disease*, *19*(1), 1–17. <https://doi.org/10.3233/JAD-2010-1221>.Alzheimer

- Nelson, P. T., Braak, H., & Markesbery, W. R. (2009). Neuropathology and cognitive impairment in Alzheimer disease: a complex but coherent relationship. *Journal of Neuropathology and Experimental Neurology*, *68*(1), 1–14.  
<https://doi.org/10.1097/NEN.0b013e3181919a48>
- Novoa, I., Zhang, Y., Zeng, H., Jungreis, R., Harding, H. P., & Ron, D. (2003). Stress-induced gene expression requires programmed recovery from translational repression. *EMBO Journal*, *22*(5), 1180–1187.  
<https://doi.org/10.1093/emboj/cdg112>
- O'Connor, T., Sadleir, K. R., Maus, E., Velliquette, R. A., Zhao, J., Cole, S. L., ... Vassar, R. (2008). Phosphorylation of the Translation Initiation Factor eIF2 $\alpha$  Increases BACE1 Levels and Promotes Amyloidogenesis. *Neuron*, *60*(6), 988–1009.  
<https://doi.org/10.1016/j.neuron.2008.10.047>
- Ohno, M. (2014). Roles of eIF2 $\alpha$  kinases in the pathogenesis of Alzheimer's disease. *Frontiers in Molecular Neuroscience*, *7*(April), 1–8.  
<https://doi.org/10.3389/fnmol.2014.00022>
- Ohoka, N., Yoshii, S., Hattori, T., Onozaki, K., & Hayashi, H. (2005). TRB3, a novel ER stress-inducible gene, is induced via ATF4-CHOP pathway and is involved in cell death. *The EMBO Journal*, *24*, 1243–1255.  
<https://doi.org/10.1038/sj.emboj.7600596>
- Ohta, K., Mizuno, A., Li, S., Itoh, M., Ueda, M., Ohta, E., ... Nakagawa, T. (2011). Endoplasmic reticulum stress enhances  $\gamma$ -secretase activity. *Biochemical and Biophysical Research Communications*, *416*(3–4), 362–366.  
<https://doi.org/10.1016/j.bbrc.2011.11.042>
- Olsson, F., Schmidt, S., Althoff, V., Munter, L. M., Jin, S., Rosqvist, S., ... Lundkvist, J. (2014). Characterization of intermediate steps in amyloid beta (A $\beta$ ) production under near-native conditions. *Journal of Biological Chemistry*, *289*(3), 1540–1550.  
<https://doi.org/10.1074/jbc.M113.498246>

- Onuki, R., Bando, Y., Suyama, E., Katayama, T., Kawasaki, H., Baba, T., ... Taira, K. (2004). An RNA-dependent protein kinase is involved in tunicamycin-induced apoptosis and Alzheimer's disease. *EMBO Journal*, *23*(4), 959–968. <https://doi.org/10.1038/sj.emboj.7600049>
- Pakos-Zebrucka, K., Koryga, I., Mnich, K., Ljubic, M., Samali, A., & Gorman, A. M. (2016). The integrated stress response. *EMBO Reports*, *17*(10), 1374–1395. <https://doi.org/10.15252/embr.201642195>
- Pavitt, G. D., Ramaiah, K. V. A., Kimball, S. R., & Hinnebusch, A. G. (1998). eIF2 independently binds two distinct eIF2b subcomplexes that catalyze and regulate guanine-nucleotide exchange. *Genes and Development*, *12*(4), 514–526. <https://doi.org/10.1101/gad.12.4.514>
- Pearson, H. A., & Peers, C. (2006). Physiological roles for amyloid  $\beta$  peptides. *Journal of Physiology*, *575*(1), 5–10. <https://doi.org/10.1113/jphysiol.2006.111203>
- Pitale, P. M., Gorbatyuk, O., & Gorbatyuk, M. (2017). Neurodegeneration: Keeping ATF4 on a Tight Leash. *Frontiers in Cellular Neuroscience*, *11*(December), 1–8. <https://doi.org/10.3389/fncel.2017.00410>
- Podust, L. M., Krezel, A. M., & Kim, Y. (2001). Crystal structure of the CCAAT box/enhancer-binding protein  $\beta$  activating transcription factor-4 basic leucine zipper heterodimer in the absence of DNA. *Journal of Biological Chemistry*, *276*(1), 505–513. <https://doi.org/10.1074/jbc.M005594200>
- Ron, D. (2002). Translational control in the endoplasmic reticulum stress response. *Journal of Clinical Investigation*, Vol. 110, pp. 1383–1388. <https://doi.org/10.1172/JCI0216784>
- Rozpedek, W., Markiewicz, L., Diehl, J. A., Pytel, D., & Majsterek, I. (2015). Unfolded Protein Response and PERK Kinase as a New Therapeutic Target in the Pathogenesis of Alzheimer's Disease. *Current Medicinal Chemistry*, *22*(27), 3169–3184.

- Rutkowski, D. T., Arnold, S. M., Miller, C. N., Wu, J., Li, J., Gunnison, K. M., ... Kaufman, R. J. (2006). Adaptation to ER stress is mediated by differential stabilities of pro-survival and pro-apoptotic mRNAs and proteins. *PLoS Biology*, 4(11), 2024–2041. <https://doi.org/10.1371/journal.pbio.0040374>
- Scheff, S. W., Price, D. A., Schmitt, F. A., & Mufson, E. J. (2006). Hippocampal synaptic loss in early Alzheimer's disease and mild cognitive impairment. *Neurobiology of Aging*, 27(10), 1372–1384. <https://doi.org/10.1016/j.neurobiolaging.2005.09.012>
- Scheuner, D., Eckman, C., Jensen, M., Song, X., Citron, M., Suzuki, N., ... Younkin, S. (1996). Secreted amyloid  $\beta$ -protein similar to that in the senile plaques of Alzheimer's disease is increased in vivo by the presenilin 1 and 2 and APP mutations linked to familial Alzheimer's disease. *12*(march), 925–928.
- Segev, Y., Barrera, I., Ounallah-Saad, H., Wibrand, K., Sporild, I., Livne, A., ... Rosenblum, K. (2015). PKR Inhibition Rescues Memory Deficit and ATF4 Overexpression in ApoE 4 Human Replacement Mice. *Journal of Neuroscience*, 35(38), 12986–12993. <https://doi.org/10.1523/jneurosci.5241-14.2015>
- Segev, Yifat, Michaelson, D. M., & Rosenblum, K. (2013). ApoE  $\epsilon$ 4 is associated with eIF2 $\alpha$  phosphorylation and impaired learning in young mice. *Neurobiology of Aging*, 34(3), 863–872. <https://doi.org/10.1016/j.neurobiolaging.2012.06.020>
- Selkoe, D. (1994). Cell Biology of the Amyloid beta-Protein Precursor and the Mechanism of Alzheimer's Disease. *Annual Review of Cell and Developmental Biology*, 10(1), 373–403. <https://doi.org/10.1146/annurev.cellbio.10.1.373>
- Steckley, D., Karajgikar, M., Dale, L. B., Fuerth, B., Swan, P., Drummond-Main, C., ... Cregan, S. P. (2007). Puma is a dominant regulator of oxidative stress induced Bax activation and neuronal apoptosis. *The Journal of Neuroscience : The Official Journal of the Society for Neuroscience*, 27(47), 12989–12999. <https://doi.org/10.1523/JNEUROSCI.3400-07.2007>



- Strittmatter, W. J., & Roses, A. D. (1997). Apolipoprotein E and disease. *Medicina Clínica, 109*(6), 216–218. Retrieved from [www.annualreviews.org](http://www.annualreviews.org)
- Szegezdi, E., Logue, S. E., Gorman, A. M., & Samali, A. (2006). Mediators of endoplasmic reticulum stress-induced apoptosis. *EMBO Reports, 7*(9), 880–885. <https://doi.org/10.1038/sj.embor.7400779>
- Takami, M., Nagashima, Y., Sano, Y., Ishihara, S., Morishima-Kawashima, M., Funamoto, S., & Ihara, Y. (2009). g-Secretase: Successive Tripeptide and Tetrapeptide Release from the Transmembrane Domain of -Carboxyl Terminal Fragment. *Journal of Neuroscience, 29*(41), 13042–13052. <https://doi.org/10.1523/jneurosci.2362-09.2009>
- Tanaka, T., Tsujimura, T., Takeda, K., Sugihara, A., Maekawa, A., Terada, N., ... Akira, S. (1998). Targeted disruption of ATF4 discloses its essential role in the formation of eye lens fibres. *Genes to Cells, 3*(12), 801–810. <https://doi.org/10.1046/j.1365-2443.1998.00230.x>
- Tong, T., Ji, J., Jin, S., Li, X., Fan, W., Song, Y., ... Zhan, Q. (2005). Gadd45a Expression Induces Bim Dissociation from the Cytoskeleton and Translocation to Mitochondria. *Molecular and Cellular Biology, 25*(11), 4488–4500. <https://doi.org/10.1128/mcb.25.11.4488-4500.2005>
- Trinh, M. A., Ma, T., Kaphzan, H., Bhattacharya, A., Antion, M. D., Cavener, D. R., ... Klann, E. (2014). The eIF2 $\alpha$  kinase PERK limits the expression of hippocampal metabotropic glutamate receptor-dependent long-term depression. *Learning and Memory, 21*(5), 298–304. <https://doi.org/10.1101/lm.032219.113>
- Tsujimoto, Y., Cossman, J., Jaffe, E., & Croce, C. M. (1985). Involvement of the bcl-2 gene in human follicular lymphoma. *Science, 228*(4706), 1440–1443. <https://doi.org/10.1126/science.3874430>

- Vallejo, M., Ron, D., Miller, C. P., & Habener, J. F. (1993). C/ATF, a member of the activating transcription factor family of DNA-binding proteins, dimerizes with CAAT/enhancer-binding proteins and directs their binding to cAMP response elements. *Proceedings of the National Academy of Sciences*, *90*(10), 4679–4683. <https://doi.org/10.1073/pnas.90.10.4679>
- Vassar, R., Kovacs, D. M., Yan, R., & Wong, P. C. (2009). The B-Secretase Enzyme BACE in Health and Alzheimer's Disease: Regulation, Cell Biology, Function, and Therapeutic Potential. *Journal of Neuroscience*, *29*(41), 12787–12794. <https://doi.org/10.1523/jneurosci.3657-09.2009>
- Vattem, K. M., & Wek, R. C. (2004). Reinitiation involving upstream ORFs regulates ATF4 mRNA translation in mammalian cells. *Proceedings of the National Academy of Sciences*, *101*(31), 11269–11274. <https://doi.org/10.1073/pnas.0400541101>
- Vaux, D. L., Cory, S., & Adams, J. M. (1988, September). Bcl-2 gene promotes haemopoietic cell survival and cooperates with c-myc to immortalize pre-B cells. *Nature*, Vol. 335, pp. 440–442. <https://doi.org/10.1038/335440a0>
- Wakabayashi, T., & De Strooper, B. (2008). Presenilins: members of the gamma-secretase quartets, but part-time soloists too. *Physiology (Bethesda, Md.)*, *23*, 194–204. <https://doi.org/10.1152/physiol.00009.2008>
- Wang, C., Huang, Z., Du, Y., Cheng, Y., Chen, S., & Guo, F. (2010). ATF4 regulates lipid metabolism and thermogenesis. *Cell Research*, *20*(2), 174–184. <https://doi.org/10.1038/cr.2010.4>
- Wei, N., Zhu, L. Q., & Liu, D. (2015). ATF4: a Novel Potential Therapeutic Target for Alzheimer's Disease. *Molecular Neurobiology*, *52*(3), 1765–1770. <https://doi.org/10.1007/s12035-014-8970-8>
- Wek, R. C., Jiang, H.-Y., & Anthony, T. G. (2006). Coping with stress: eIF2 kinases and translational control. *Biochemical Society Transactions*, *34*(1), 7–11. <https://doi.org/10.1042/BST0340007>

- Willis, S. N., Fletcher, J. I., Kaufmann, T., Van Delft, M. F., Chen, L., Czabotar, P. E., ... Huang, D. C. S. (2007). Apoptosis initiated when BH3 ligands engage multiple Bcl-2 homologs, not Bax or Bak. *Science*, *315*(5813), 856–859.  
<https://doi.org/10.1126/science.1133289>
- Wortel, I. M. N., van der Meer, L. T., Kilberg, M. S., & van Leeuwen, F. N. (2017). Surviving Stress: Modulation of ATF4 Mediated Stress Responses in Normal and Malignant Cells. *Trends in Endocrinology & Metabolism*, *28*(11).
- Xu, S., Di, Z., He, Y., Wang, R., Ma, Y., Sun, R., ... Shen, Y. (2019). Mesencephalic astrocyte-derived neurotrophic factor (MANF) protects against A $\beta$  toxicity via attenuating A $\beta$ -induced endoplasmic reticulum stress. *Journal of Neuroinflammation*, *16*(1). <https://doi.org/10.1186/s12974-019-1429-0>
- Yang, X., Matsuda, K., Bialek, P., Jacquot, S., Masuoka, H. C., Schinke, T., ... Karsenty, G. (2004). ATF4 is a substrate of RSK2 and an essential regulator of osteoblast biology; implication for Coffin-Lowry Syndrome. *Cell*, *117*(3), 387–398. Retrieved from <http://www.ncbi.nlm.nih.gov/pubmed/15109498>
- Yasojima, K., Akiyama, H., McGeer, E. G., & McGeer, P. L. (2001). Reduced neprilysin in high plaque areas of Alzheimer brain: A possible relationship to deficient degradation of  $\beta$ -amyloid peptide. *Neuroscience Letters*, *297*(2), 97–100.  
[https://doi.org/10.1016/S0304-3940\(00\)01675-X](https://doi.org/10.1016/S0304-3940(00)01675-X)
- Ye, J., Kumanova, M., Hart, L. S., Sloane, K., Zhang, H., De Panis, D. N., ... Koumenis, C. (2010). The GCN2-ATF4 pathway is critical for tumour cell survival and proliferation in response to nutrient deprivation. *EMBO Journal*, *29*(12), 2082–2096. <https://doi.org/10.1038/emboj.2010.81>
- Youle, R. J., & Strasser, A. (2008). The BCL-2 protein family: Opposing activities that mediate cell death. *Nature Reviews Molecular Cell Biology*, *9*(1), 47–59.  
<https://doi.org/10.1038/nrm2308>
- Young, S. K., & Wek, R. C. (2016). Upstream open reading frames differentially regulate genespecific translation in the integrated stress response. *Journal of Biological Chemistry*, *291*(33), 16927–16935. <https://doi.org/10.1074/jbc.R116.733899>

Zha, H., Aimé-Sempé, C., Sato, T., & Reed, J. C. (1996). Proapoptotic protein Bax heterodimerizes with Bcl-2 and homodimerizes with Bax via a novel domain (BH3) distinct from BH1 and BH2. *Journal of Biological Chemistry*, 271(13), 7440–7444. <https://doi.org/10.1074/jbc.271.13.7440>

## Appendices

### Appendix A: ATF4 genotyping primers

Wildtype Forward	AGCAAAACAAGACAGCAGCCACTA
Knockout Forward	ATATTGCTGAAGAGCTTGGCGGC
Common Reverse	GTTTCTACAGCTTCCTCCACTCTT

**Appendix B: PUMA genotyping primers**

Primer 1	AGGCTGTCCCTGGGGTCATCCC
Primer 2	GGACTGTGCGGGGCTAGACCCTCTG
Primer 3	ACCGCGGGCTCCGAGTAGC

**Appendix C: List of qRT-PCR primers**

Gene	Forward Sequence	Reverse Sequence
4eBP1	GGGGACTACAGCACCCTC	GTTCCGACACTCCATCAGAAAT
CHOP	ACAGAGGTCACACGCACATC	GGGCACTGACCACTCTGTTT
Gadd45 $\alpha$	CTGCTGCTACTGGAGAACGAC	CGACTTTCCCGGCAAAAACAAA
PUMA	CCTCAGCCCTCCCTGTCACCAG	CCGCCGCTCGTACTGCGCGTTG
S12	GGAAGGCATAGCTGCTGG	CCTCGATGACATCCTTGG
Trib3	TGCAGGAAGAAACCGTTGGAG	CTCGTTTTAGGACTGGACACTT

## Curriculum Vitae

**Name:** Gillian Petroff

**Post-secondary Education and Degrees:** The University of Western Ontario  
London, Ontario, Canada  
2013-2017 B.Sc.

The University of Western Ontario  
London, Ontario, Canada  
2017-2019 M.Sc.

**Honours and Awards:** The Western Scholarship of Distinction  
The University of Western Ontario  
2013

Western Graduate Research Scholarship  
The University of Western Ontario  
2017-2019

**Related Work Experience** Physiology and Pharmacology Teaching Assistant  
The University of Western Ontario  
PhysPharm 3000E 2017-2018  
PhysPharm 3000E 2018-2019